Synextensional Granitoids and Detachment Systems Within Cycladic Metamorphic Core Complexes (Aegean Sea, Greece): Toward a Regional Tectonomagmatic Model

Aurélien Rabillard, Laurent Jolivet, Laurent Arbaret, Eloïse Bessière, Valentin Laurent, Armel Menant, Romain Augier, Alexandre Beaudoin

AGU100 ADVANCING EARTH AND SPACE SCIENCE

Tectonics

RESEARCH ARTICLE
10.1029/2017TC004697

Special Section:
Geodynamics, Crustal and Lithospheric Tectonics, and active deformation in the Mediterranean Regions (A tribute to Prof. Renato Funiciello)

Synextensional Granitoids and Detachment Systems Within Cycladic Metamorphic Core Complexes (Aegean Sea, Greece): Toward a Regional Tectonomagmatic Model

Aurélien Rabillard[1,2,3], Laurent Jolivet[4], Laurent Arbaret[1,2,3], Eloïse Bessière[1,2,3], Valentin Laurent[1,2,3], Armel Menant[5], Romain Augier[1,2,3], and Alexandre Beaudoin[1,2,3]

[1]Université d'Orléans, ISTO, UMR 7327, Orléans, France, [2]CNRS/INSU, ISTO, UMR 7327, Orléans, France, [3]BRGM, ISTO, UMR 7327, Orléans, France, [4]CNRS-INSU, Institut des Sciences de la Terre Paris, ISTeP UMR 7193, Sorbonne Université, Paris, France, [5]Institut de Physique du Globe de Paris, Paris Sorbonne Cité, University Diderot, UMR 7154-CNRS, Tectonique et Mécanique de la Lithosphère, Paris, France

Key Points:
- Kinematic and dynamic links of synextensional magmatism and detachment faulting in Cycladic metamorphic core complexes are described
- Dome exhumations achieved below single system of detachments progressively inactivated and replaced by new upper detachments during intrusion
- Newly formed detachments are expressed within granitoids through continuum of deformation from magmatic to ductile-then-brittle conditions

Correspondence to:
L. Jolivet,
laurent.jolivet@sorbonne-universite.fr

Citation:
Rabillard, A., Jolivet, L., Arbaret, L., Bessière, E., Laurent, V., Menant, A., et al. (2018). Synextensional granitoids and detachment systems within Cycladic metamorphic core complexes (Aegean Sea, Greece): Toward a regional tectonomagmatic model. *Tectonics*, *37*. https://doi.org/10.1029/2017TC004697

Received 16 JUN 2017
Accepted 1 JUL 2018
Accepted article online 6 JUL 2018

Abstract Within deforming continental regions where metamorphic core complexes (MCCs) and synextensional granitoids are closely associated, deciphering the link between detachment faulting and magmatism often remains complex as (1) the rheological weakness of magma may stimulate mechanisms of strain localization, and conversely, (2) tectonic processes may open/close drains where magmas can intrude. Here we tackle this issue by focusing on the Cyclades with the comparison of five granitoid-cored MCCs (Tinos, Mykonos, Ikaria, Naxos, and Serifos) and their flanking detachment systems. In this region, granitoids were emplaced into the middle/upper crust over a relatively short time period (15–9 Ma), while metamorphic domes were largely exhumed after more than 10 Myr of extension. None of those intrusions thereby proves to be a real candidate for the genesis of MCCs but would rather be a consequence of a warmer regime during lithospheric thinning. However, all collected structural and kinematic data converge toward a regional scheme in which magmatic activity played a more pivotal role than previously postulated. Indeed, late evolution stages of MCCs were dynamically impacted by intrusions along which local and transient heterogeneities of the mechanical strength occurred, interfering with the sequential development of detachments. During their tectonically controlled emplacement, magmatic products intruded already formed detachments at depth, locally inhibiting their activity, associated with a contemporaneous upward migration of extensional deformation that tended to localize through time within intrusion roofs along rheological discontinuities. The newly formed detachments are expressed within granitoids through a continuum of deformation from comagmatic to ductile conditions, followed by cataclasis along detachments.

Plain Language Summary Tectonics intensely deform continents forming mountains when the crust is thickened or low-standing regions where the sea can invade in the case of extension. Extension is less spectacular as deformation is hidden below sea level, but it involves intense deformations that can be studied when the deep crustal levels are exhumed below extensional faults with low-angle detachments. The portions of exhumed crust reveal deep deformation processes associated with emplacement of magmatic rocks because extension is coeval with heat advection toward the surface. One long pending question is whether or not the evolution of these detachments is influenced by growing granites. Based on a detailed field study of the deformation of five such examples in the Cycladic Archipelago, we show that the granites modify the evolution of the low-angle extensional faults leading to the sequential development and upward migration in the crust of a series of detachments through time. Granites indeed influence the evolution of detachments because they heat the crust in their vicinity and thus modify its mechanical resistance and introduce a mechanical heterogeneity during growth and cooling as the magma is intrinsically weak. The flow of magma in these granitic bodies is in turn influenced by tectonic forces.

1. Introduction

Within highly extended continental domains, the development of metamorphic core complexes (MCCs) represents one of the most effective mechanisms for rapid exhumation of deep-seated materials toward upper crustal levels. Historically described in the North American Cordillera (Crittenden et al., 1980; Davis &

Coney, 1979) and then evidenced in the Mediterranean Region (Avigad & Garfunkel, 1989; Lister et al., 1984) or in East Asia (Davis et al., 1996; Faure et al., 1996; Jolivet et al., 1999), MCCs are classically regarded as dome-like structures roofed by a single detachment or, in more complex ways, by multiple and closely spaced detachments (Lister & Davis, 1989; Spencer, 1984). Usually associated with normal sense displacements of several tens of kilometers, MCC-bounding detachments are thick ductile shear zones in the deep crust that evolve into brittle low-angle normal faults in the upper crust (see recent reviews by Platt et al., 2015; Whitney et al., 2013). In addition to an upward mass transfer, crustal thinning and formation of MCCs are often coupled with partial melting of the upper mantle and/or the lower crust as well as conductive heat dissipation toward the Earth's surface, giving rise to complex spatiotemporal interrelations between intrusive magmatism and active detachment zones at various crustal levels (Vanderhaeghe, 2009; Vanderhaeghe & Teyssier, 2001; Whitney et al., 2004). Well documented by field-based contributions worldwide, granitoid-cored MCCs have been, for instance, widely recognized in the North American Cordillera (Armstrong & Ward, 1991; Campbell-Stone et al., 2000; Dallmeyer et al., 1986; Davis & Coney, 1979; Hyndman, 1980; Vanderhaeghe & Teyssier, 1997), in East Asia (Charles et al., 2013, 2011; Davis et al., 1996; Faure et al., 1996; Lin & Wang, 2006; Shu et al., 1998; Webb et al., 1999), in the Mediterranean region (Bozkurt & Park, 1994; Daniel & Jolivet, 1995; Dinter & Royden, 1993; Faccenna et al., 1999; Hetzel et al., 1995; Jolivet et al., 1990, 1998; Whitney & Dilek, 1997), and particularly in the Aegean Sea (Greece) where some of the metamorphic domes and their flanking detachment systems developed in close association with plutonic intrusions (Beaudoin et al., 2015; Denèle et al., 2011; Faure et al., 1991; Gautier et al., 1993; Grasemann & Petrakakis, 2007; Jolivet et al., 2010, 2015; Laurent et al., 2015; Lee & Lister, 1992; Rabillard et al., 2015).

Over the past four decades, studies thus partly focused on assessing geological processes through which MCC-bounding detachments could have been geometrically and kinematically paired with short-lived magmatic episodes during a protracted exhumation history. In particular, the causal link between both phenomena was vigorously discussed and this debate still continues as far as different conceptual models are conceivable depending on whether plutonic activity slightly predates, coincides, postdates, and/or punctuates extension. A commonly held model suggests that preextensional to synextensional magmatism could embody a prominent catalyst agent for orogenic collapse and a sufficient trigger to form MCCs (Baldwin et al., 1993; Carr, 1992; Hill et al., 1995). Within the lower and middle crust, the heat flux and accumulation of melting products can indeed transiently introduce a drastic thermal weakening of surrounding rocks, promoting a lateral spreading of the orogenic wedge and an upward ductile flow of the dome-shaped partially molten lower crust (Armstrong, 1982; Augier, Choulet, et al., 2015; Brown & Dallmeyer, 1996; Coney & Harms, 1984; Gans, 1987; MacCready et al., 1997; Vanderhaeghe, 2012; Vanderhaeghe & Teyssier, 2001). At a more restricted scale, unconsolidated individual intrusions, as parts of larger plutons, are capable to generate strong rheological heterogeneities along which the onset of extensional shearing and subsequent mechanisms of strain localization can be efficiently stimulated (Brun & Van Den Driessche, 1994; Lynch & Morgan, 1987; Pavlis, 1996). Expansion of overpressured magmas or a rapidly growing pluton by repeated magma injections may further destabilize over a short time period the ambient stress field by deflecting the maximum principal stress axis away from vertical, thereby favoring a strain accommodation through low-dipping normal faults above intrusive zones (Parsons & Thompson, 1993; Vigneresse et al., 1999). Alternatively, when lithospheric thinning appears to be already initiated prior to intrusive magmatism, it was often argued that late orogenic to postorogenic extensional exhumations below crustal-scale detachments could set off a decompression-driven partial melting of the deep lithosphere and an extraction of magmatic pulses toward shallower crustal levels (Teyssier et al., 2005; Teyssier & Whitney, 2002; Whitney et al., 2004). In cooperation with various ascent mechanisms, magma migration through the crust can be partly guided by local pressure gradients induced by high-shear strain zones, as far as reaching major detachment faults acting as mechanical boundaries for magma storage (Bonini et al., 2001; Fletcher et al., 1995; Vanderhaeghe, 1999). Once accumulated into deforming zones, partially crystallized magmas can in turn temporarily disturb both the thermal structure and the deformational regime prevailing within the surrounding system. As a result, magmas may strongly modify the style and pattern of faulting such as the upward arching of preexisting detachment surfaces or even the sequential development of localizing events involving a polyphased faulting history (Daniel & Jolivet, 1995; Davis et al., 1993; Lister & Baldwin, 1993).

Testing these interrelations at local and regional scales requires a multidisciplinary approach to constrain (1) the relative timing between magmatism, strain localization, and related contact metamorphism; (2)

the geometrical relations between granitoids and large-scale tectonic structures; and (3) the distribution and evolution of deformation fossilized inside and outside granitoids. In this perspective, the Cyclades prove to be a valuable natural laboratory since thermochronological investigations have clearly shown that several I- and S-type intrusions were emplaced alongside detachment faults during the late exhumation stage of metamorphic domes (Bolhar et al., 2010; Brichau et al., 2008, 2007; Iglseder et al., 2009; Keay, 1998; Keay et al., 2001). Despite these meaningful progresses on the geological understanding of the Cyclades, no consensus has yet been reached on the mechanisms responsible for the observed relations between the Cycladic plutons and the associated detachments. Indeed, most contributions have concluded that the late plutonic stage appears to be neither a major trigger for the development of MCCs nor a strong helper for strain localization along flanking detachments, and some of them would have merely acted as passive markers of crustal extension (Bolhar et al., 2010; Brichau et al., 2008, 2007). In this sense, extensional deformation would have rather promoted preferential pathways for magma transport through the crust, while the location of pluton emplacement would be controlled by active detachments (Bolhar et al., 2010). Though acknowledging the logic of this latter proposal, some field-based studies have alternatively suggested a more pivotal role of the plutonic activity in redistribution and localization of extensional deformation by promoting the development of new detachment zones (Bessière et al., 2017; Denèle et al., 2011; Jolivet et al., 2010; Laurent et al., 2015; Rabillard et al., 2015). Otherwise, a few studies have proposed the preeminent role of transtensional or transpressional strike-slip faults for both the emplacement of those granitoids and ensuing deformation (Boronkay & Doutsos, 1994; Koukouvelas & Kokkalas, 2003).

In the present paper we therefore synthetize key tectonometamorphic and geochronological data related to the development of the Cycladic MCCs where detachment systems were closely associated with granitoids, as well as new structural data we collected from those intrusions. As a result of this review, we propose a regional scheme in which magmatic complexes dynamically impacted the development of MCCs rather than their passive attitude with regard to extensional tectonics.

2. Geodynamic and Geological Context of the Aegean Region With Focus on the Cyclades

The Aegean region, that is, the easternmost Mediterranean back-arc domain, was formed in the overriding plate of the retreating Hellenic subduction zone (Le Pichon & Angelier, 1981a, 1981b; Royden, 1993). As most extending continental domains, the Aegean region experienced a protracted tectonic history that has produced thermomechanical heterogeneities in the crust, for example, large thrusts, synorogenic detachments, partial melting zones, or even intrusions (Jolivet & Brun, 2010; Royden & Papanikolaou, 2011). Driven by the convergence between Africa and Eurasia since the Mesozoic, the Aegean back-arc domain was previously occupied by the Hellenides-Taurides belt, a polygenic orogenic wedge built up by the successive accretion of both oceanic and continental upper crustal units (Aubouin, 1959; Bonneau, 1984; Jacobshagen et al., 1978; Ring et al., 2010; van Hinsbergen et al., 2005). The resulting SW verging nappe stacking has thus triggered successively burial and synorogenic exhumation processes in high-pressure-low-temperature (H*P*-L*T*) metamorphic conditions below crustal-scale thrusts and synorogenic detachments, respectively (Brun & Faccenna, 2008; Huet et al., 2009; Jolivet et al., 1994, 2003; Laurent et al., 2016; Ring, Glodny, et al., 2007; Ring, Will, et al., 2007). From the Early Eocene onward (~45 Ma), the Hellenic overthickened crust was first subjected to extensional tectonics by a possible lithospheric delamination while the Hellenic subduction zone remained relatively static or retreated slowly southward, thus allowing the development of the Rhodope MCCs in the northernmost Aegean (Burg, 2012). In response to a faster backward retreat of the north dipping Hellenic slab since 35–30 Ma, the subduction front was increasingly dragged southward and the Eurasian upper plate underwent extensional collapse in back-arc domain (Jolivet & Faccenna, 2000), until reaching the present-day tectonic architecture of the Aegean domain with an arcuate accretionary wedge (i.e., the Mediterranean Ridge, Figure 1a). Back-arc active extension is mainly circumscribed around the Aegean Sea, that is, Western Turkey, the Corinth rift, the southern Peloponnese, and Crete (Goldsworthy et al., 2002; Hatzfeld et al., 2000; Jackson, 1994). The almost total lack of seismic activity in the Cycladic Archipelago, only present below the southern Aegean arc volcanoes (Bohnhoff et al., 2006, 2004; Dimitriadis et al., 2009), suggests that this region currently behaves as a rigid block.

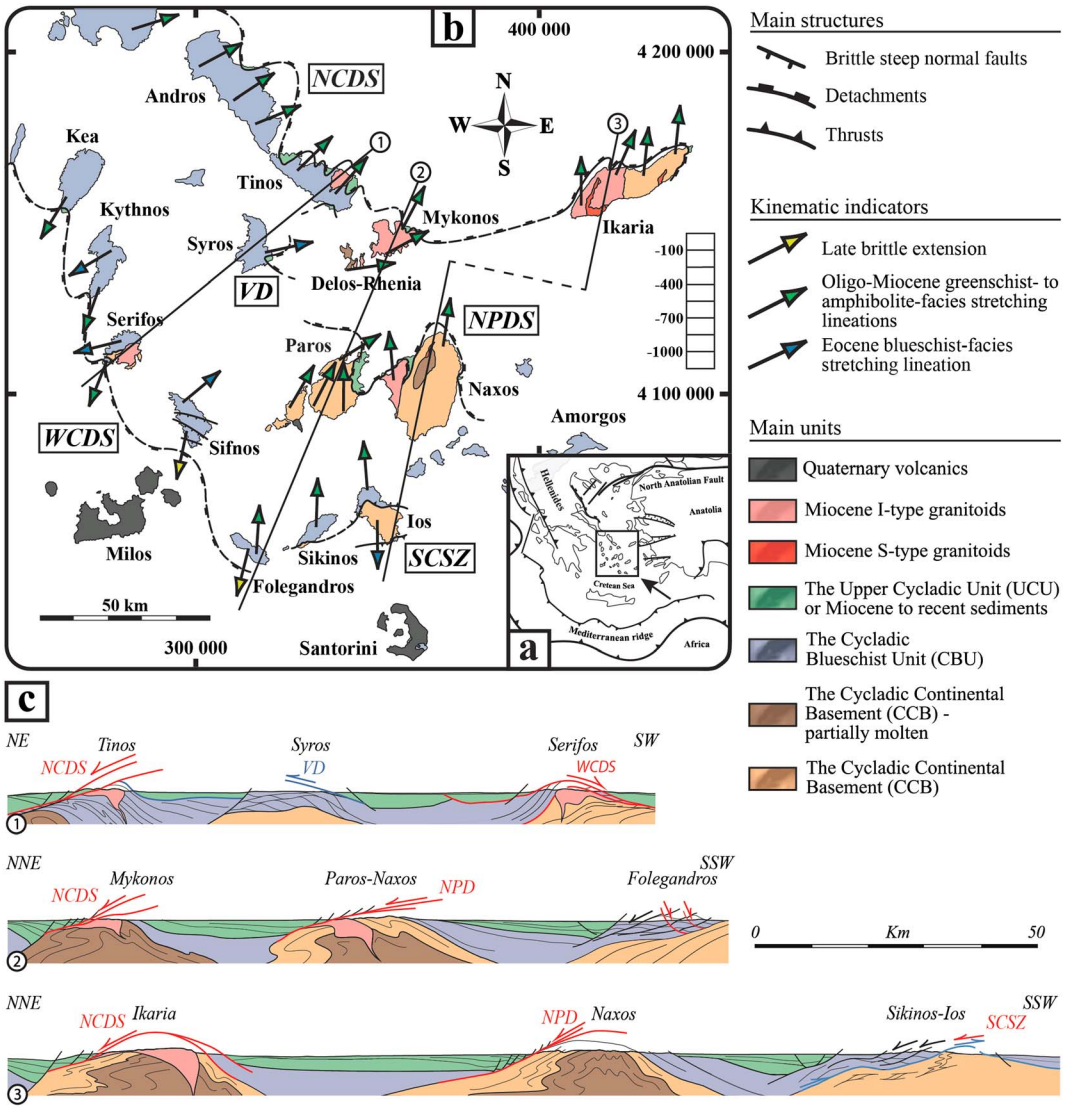

Figure 1. (a) Simplified tectonic map of the Aegean domain and location of the studied area. (b) Tectonic map of the Cyclades, modified after Huet et al. (2009), Jolivet et al. (2010, 2015), Grasemann et al. (2012), and Augier, Jolivet, et al. (2015). Coordinates on the map, including the following ones, are given in universal time meridian zone 35°N, World Geodetic System (WGS) 1984. At regional scale, note the spatial interaction between I-type granitoids (Tinos, Mykonos-Delos-Rhenia, Ikaria, Naxos, and Serifos Islands) and metamorphic core complexes together with their flanking detachments. (c) Cross sections through the Cyclades (1–3), modified after Augier, Jolivet, et al. (2015). Sections are roughly parallel to the tectonic transport and highlight the close interaction between granitoids and detachments. NCDS = North Cycladic Detachment System; NPDS = Naxos-Paros Detachment System; WCDS = West Cycladic Detachment System; SCSZ = South Cyclades Shear Zone; VD = Vari detachment.

In the Cycladic archipelago, located in the central Aegean Sea, back-arc extension was active from the Late Oligocene to the Late Miocene (Jolivet & Brun, 2010; Jolivet & Faccenna, 2000; Ring et al., 2010). During this period, slab rollback and related change of stress regime were presumably accompanied with a lithospheric delamination and a slab tear, all of that being also coeval with a warmer thermal state in the lithosphere, partial melting of the extending lower crust, and the formation of multiple MCCs (Ersoy & Palmer, 2013; Gautier & Brun, 1994a, 1994b; Gautier et al., 1993; Keay et al., 2001; Lister et al., 1984; Menant, Jolivet, & Vrielynck, 2016; Menant, Sternai, et al., 2016; Pe-Piper & Piper, 2006; Vanderhaeghe, 2004). More specifically, the development of the Cycladic MCCs and their affiliated crustal-scale detachments led to progressive exhumation of the deepest parts of the Hellenic orogenic wedge (i.e., the Cycladic Continental Basement [CCB] and the Cycladic Blueschist Unit [CBU], see thereafter) under greenschist- to amphibolite-facies retrograde metamorphism

that partly overprinted a former Eocene subduction-related H*P*-L*T* metamorphism evidenced by relics of eclogite and blueschist parageneses (Avigad et al., 1997; Buick, 1991a, 1991b; Jansen, 1977; Jolivet & Patriat, 1999; Urai et al., 1990). In the northern and central Cyclades, extensional exhumation was respectively achieved below the North Cycladic Detachment System (NCDS, Figures 1b and 1c; Jolivet et al., 2010; Lecomte et al., 2010) and the Naxos-Paros Detachment System (NPDS, Figures 1b and 1c; Brichau et al., 2006; Gautier et al., 1993), two sets of crustal-scale detachments with stable top-to-the-north or top-to-the-NE kinematics. At the Aegean scale, the NCDS has been tentatively extended over 200 km long from Evia to the northernmost Cycladic Islands (Andros, Tinos, and Mykonos), and even farther east on Ikaria Island (Beaudoin et al., 2015; Jolivet et al., 2010). In the Western Cyclades, a large part of the extensional exhumation was accommodated by the West Cycladic Detachment System (WCDS, Figures 1b and 1c), a series of opposite top-to-the-SW detachments that crop out along a discontinuous 100-km-long trend from Lavrion (Greece mainland; Berger et al., 2013; Krohe et al., 2010; Lekkas et al., 2011; Skarpelis, 2007) to the westernmost Cycladic Islands (Kythnos, Kea, and Serifos; Grasemann et al., 2012; Iglseder et al., 2011; Rice et al., 2012). A possible southeastward extension of the WCDS has been proposed offshore south of Sifnos and Folegandros Islands on which south oriented, late brittle displacements have been described (Augier, Jolivet, et al., 2015; Ring et al., 2011; Roche et al., 2016). Farther east on Sikinos and Ios Islands, a localized top-to-the-south shearing has been also recognized (Figures 1b and 1c), initially interpreted as an extensional shear zone (i.e., the South Cyclades Shear Zone; Baldwin & Lister, 1998; Foster & Lister, 2009; Lister et al., 1984; Vandenberg & Lister, 1996) but later viewed as an Eocene H*P*-L*T* event of thrusting, reworked afterward by a top-to-the-north extensional deformation since Oligocene time (Augier, Jolivet, et al., 2015; Huet et al., 2009).

Final exhumation was mainly completed by brittle increments of deformation along detachments, bringing back toward the surface three main units (Bonneau, 1984; Jolivet & Brun, 2010; Jolivet, Famin, et al., 2004; Ring et al., 2010). From bottom to top of the rearranged Eocene nappe stack, it has been recognized (1) the CCB, primarily made up of paragneissic and orthogneissic rocks equilibrated in the amphibolite-facies conditions of Variscan or even pre-Variscan age (Andriessen et al., 1987; Henjes-Kunst & Kreuzer, 1982; Keay & Lister, 2002). Well exposed in some tectonic windows (i.e., Naxos, Paros, Ikaria, Ios, Sikinos, Serifos, and Mykonos-Delos), the Cycladic basement further contains locally a marble-metapelite cover (Beaudoin et al., 2015; Dürr et al., 1978; Grasemann & Petrakakis, 2007; Ring et al., 1999). The CCB tectonically underlies the (2) CBU, a metavolcanosedimentary unit dominated by interlayered schists and marbles with embedded metabasite boudins (Avigad & Garfunkel, 1989; Blake et al., 1981; Keiter et al., 2004; Reinecke et al., 1982). While both the CCB and CBU were subjected to a H*P*-L*T* event during the Eocene (Andriessen et al., 1979; Bröcker et al., 1993; Groppo et al., 2009; Huet et al., 2015; Laurent et al., 2017; Maluski et al., 1987; Parra et al., 2002; Trotet et al., 2001; Wijbrans & McDougall, 1986, 1988), the overlying (3) Upper Cycladic Unit (UCU, thereafter) is devoid of synsubduction H*P* imprint, suggesting that it was not buried in the Hellenic subduction zone. Lithologically heterogeneous, the UCU crops out as small klippes. It includes a continental basement (amphibolites and gneisses) that preserves Late Cretaceous high-temperature (H*T*) metamorphic ages and a Permian to Mesozoic sedimentary cover topped by ophiolites (i.e., serpentinites, gabbros, and basalts) obducted in the Late Jurassic or Late Cretaceous (Altherr et al., 1994; Katzir et al., 1996; Martha et al., 2016; Papanikolaou, 2009; Patzak et al., 1994). This disrupted Eocene nappe stack is frequently bounded by sedimentary basins filled with Miocene to Present detrital shallow marine and continental deposits (Bargnesi et al., 2013; Kuhlemann et al., 2004; Sanchez-Gomez et al., 2002). Clasts from the underlying Cycladic units are observed indicating syntectonic deposition of sediments during footwall denudation (Bargnesi et al., 2013; Kuhlemann et al., 2004; Lecomte et al., 2010).

During the extension-related exhumation of the CCB and CBU, several syntectonic granitoids have successively intruded the Cycladic MCCs at middle/upper crustal depths (Bröcker & Franz, 1994; Cao et al., 2017; Gautier et al., 1993; Laurent et al., 2015; Lucas, 1999; Pe-Piper, 2000; St. Seymour et al., 2009). Precise zircon (U-Th)/Pb ages from those granitoids have thus revealed crystallization histories ranging from 15 to 9 Ma (Figure 2; Bargnesi et al., 2013; Bolhar et al., 2010; Brichau et al., 2008, 2007; Iglseder et al., 2009; Keay, 1998; Keay et al., 2001), a relatively short time interval during which both I- and S-type intrusions migrated from the north-northeastern Cyclades (Tinos, Mykonos-Delos, and Ikaria) to the southwest (Serifos), passing across the central Cyclades (Naxos and Paros). S-type granites were mostly linked to migmatite-cored MCCs and almost systematically older than spatially associated I-type granitoids in the examples we have studied (Figures 2). Voluminous I-type granitoids were especially emplaced alongside crustal-scale detachments and

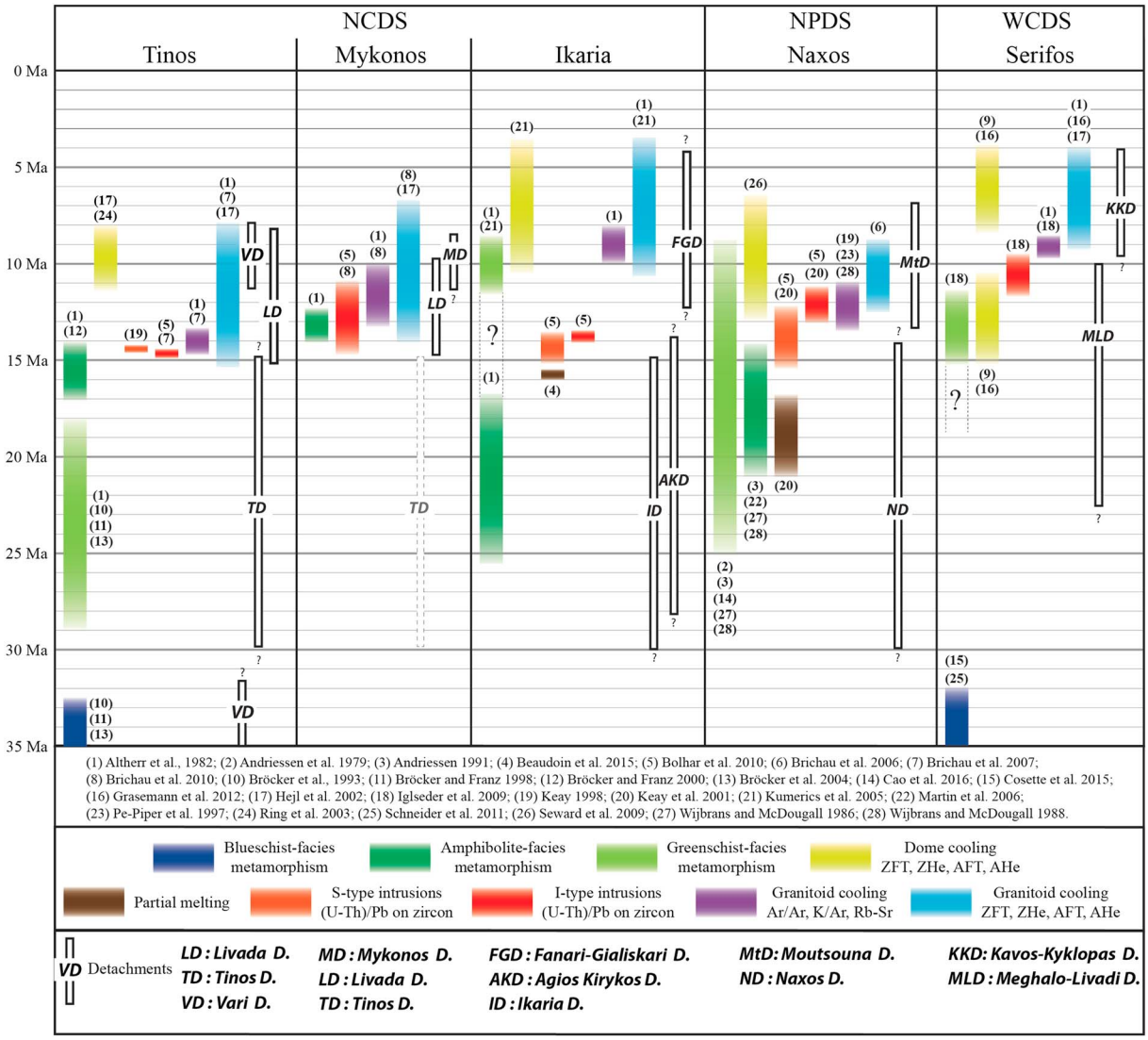

Figure 2. Compilation of available radiometric ages from the Cycladic Islands (Tinos, Mykonos-Delos-Rhenia, Ikaria, Naxos, and Serifos) where development of metamorphic core complexes and associated detachment systems (i.e., NCDS, NPDS, and WCDS) were paired with plutonic activity. The activity of the different detachments discussed in the text is shown also. See text for further information. NCDS = North Cycladic Detachment System; NPDS = Naxos-Paros Detachment System; WCDS = West Cycladic Detachment System.

have recorded the same shearing direction and sense as the host rocks (Figure 1c; Denèle et al., 2011; Faure et al., 1991; Grasemann et al., 2012; Laurent et al., 2015; Lee & Lister, 1992; Rabillard et al., 2015). I-type granitoids encompass a broad range of modal compositions, and some of them constitute composite large-scale intrusions (Altherr et al., 1982; Altherr & Siebel, 2002; Denèle et al., 2011; Iglseder et al., 2009; Pe-Piper et al., 1997). These intrusive bodies typically originated from a mixing between a crustal melting and seemingly mantle-derived magmas in fluctuating proportions, as documented by geochemical studies (Altherr et al., 1982; Altherr & Siebel, 2002; Bolhar et al., 2012; Pe-Piper & Piper, 2006; Stouraiti et al., 2010). In the field, remnants of the presumed mantle source and the significant interaction of compositionally heterogeneous magmas during cooling of the intrusions are further supported by common occurrences of mafic enclaves and dikes within more felsic plutonic bodies (Avigad et al., 1998; Denèle et al., 2011; Koukouvelas & Kokkalas, 2003; Laurent et al., 2015; Rabillard et al., 2015). Accordingly, variation in their petrological and geochemical characteristics led some authors to involve an incremental growing of plutons by multiple and discrete magma pulses, which is supported by high-resolution zircon (U-Th)/Pb geochronology reporting complex and multimodal age spectra from those I-type granitoids over few million years (Bolhar et al., 2010; Bolhar et al., 2012; de Saint Blanquat et al., 2011; Habert, 2004).

3. Detachment Systems and Synextensional Intrusions Within the Cycladic MCCs

In this section, we focus on Cycladic MCCs where crustal-scale detachment systems and I-type granitoids are closely associated (i.e., Tinos, Mykonos-Delos-Rhenia, Ikaria, Naxos, and Serifos Islands) and we report the main tectonometamorphic features related to the activity of detachment systems. A special attention is further paid to the spatiotemporal interactions between those detachment systems and plutonism.

3.1. Tinos and Mykonos-Delos-Rhenia Islands

One of the most prominent tectonic responses to the Aegean crustal extension has been particularly recognized over Tinos and Mykonos-Delos-Rhenia Islands since the development of these MCCs has been resolved into a coherent tectonic evolution involving three main branches of the NCDS, that is, the Tinos, Livada, and Mykonos detachments (Jolivet et al., 2010). Associated with a constant NE directed noncoaxial extensional deformation during the Oligo-Miocene exhumation history, these three detachments accommodated at least 70 km of displacement and reactivated/reworked successively former crustal-scale heterogeneities, suggesting a long-lasting tectonic evolution (Brichau et al., 2008; Jolivet et al., 2010).

The structurally lowermost branch, that is, the Tinos detachment, can be followed along the northeastern coast of Tinos where it unroofs a metamorphic dome elongated perpendicular to the NE directed regional extension (Figure 3a and in the included map inset at upper right). This sharp, corrugated, and shallow NE dipping normal fault, with dip angles ranging from 15° to 35°, brought in contact the UCU above the CBU (Figure 4a; Avigad & Garfunkel, 1989; Jolivet, Famin, et al., 2004; Jolivet & Patriat, 1999). As described by previous structural fieldworks, the Tinos detachment acted in the ductile-then-brittle field (Gautier & Brun, 1994b, 1994a; Jolivet, Famin, et al., 2004; Mehl et al., 2005). Below the detachment plane, rocks derived from the underlying CBU were extensively mylonitized under a progressive northeastward and upward strain gradient. Mylonitization was coeval with an intense metamorphic retrogression into the greenschist facies (Gautier & Brun, 1994b, 1994a; Parra et al., 2002) leaving well-preserved Eocene H*P*-L*T* parageneses into the deepest exposed parts of the metamorphic sequence (Bröcker et al., 1993; Bröcker et al., 2004; Bröcker & Franz, 1998; Parra et al., 2002). Locally, basal rocks of the upper unit recorded a similar top-to-the-NE shearing within a thin zone that never exceeds 100 m (Zeffren et al., 2005). Close to the detachment plane, ductile shearing both in the lower and upper unit was intersected by sets of NW-SE striking, high- and low-angle normal faults and the tectonic contact itself lies beneath a several meter thick level of faulted talc-rich breccias and noncohesive cataclasites (Figure 4a; Mehl et al., 2005; Patriat & Jolivet, 1998). Besides, geochronological analyses ascribed to the greenschist ductile exhumation yielded Oligo-Miocene ages from approximately 29 to 18 Ma (Figure 2; Altherr et al., 1982; Bröcker et al., 2004, 1993; Bröcker & Franz, 1998), showing that the Tinos detachment was predominantly active in the ductile field and ended as a brittle detachment before it was pierced and locally inactivated by the intrusive magmatic complex and associated dike arrays circa 15–14 Ma (Figures 2 and 3a; Bolhar et al., 2010; Brichau et al., 2007; Keay, 1998). Field relations along the eastern contact at Livada Beach show the intrusion of the granite within the strongly foliated and lineated greenschist-facies and amphibolite-facies metabasites of the upper unit (Jolivet & Patriat, 1999). The Tinos magmatic complex further produced a thermal overprint and consequently a well-developed contact aureole, inducing a partial to complete reset of greenschist-facies recrystallization ages that range from approximately 17 to 14 Ma (Figure 2; Altherr et al., 1982; Bröcker & Franz, 1998, 2000). A tectonic contact between the UCU and CBU is also mapped on the southern tip of Tinos (Figures 1b, 1c, and 3a). At variance with the Tinos detachment, this gently SW dipping discontinuity immediately occurs on top of blueschists and eclogites with Eocene metamorphic ages (Bröcker, 1990; Bröcker & Franz, 1998; Bröcker et al., 1993; Jolivet & Patriat, 1999; Parra et al., 2002). On account of these tectonometamorphic features, this crustal-scale structure has been rather considered as a synorogenic Eocene detachment that led to exhume the CBU in the subduction channel, better known as the Vari detachment (Jolivet et al., 2010). However, Ring et al. (2003) pointed out a strong brittle-cataclastic deformation throughout its exposure and have suggested its late reactivation in the brittle crust at approximately 11–8 Ma based on zircon and apatite (U-Th)/He L*T* thermochronology (Figure 2). This was confirmed by Soukis and Stöckli (2013) in south Syros with structural data corroborated by U-Th/He zircon and apatite ages.

At the northeastern tip of Tinos Island where the main intrusion is locally surrounded by the UCU (Livada Bay, location in Figure 3a), host metamorphic rocks display a well-developed NW striking tectonic foliation with a conspicuous NE trending stretching lineation and discrete top-to-the-NE shear bands (Brichau et al., 2007; de

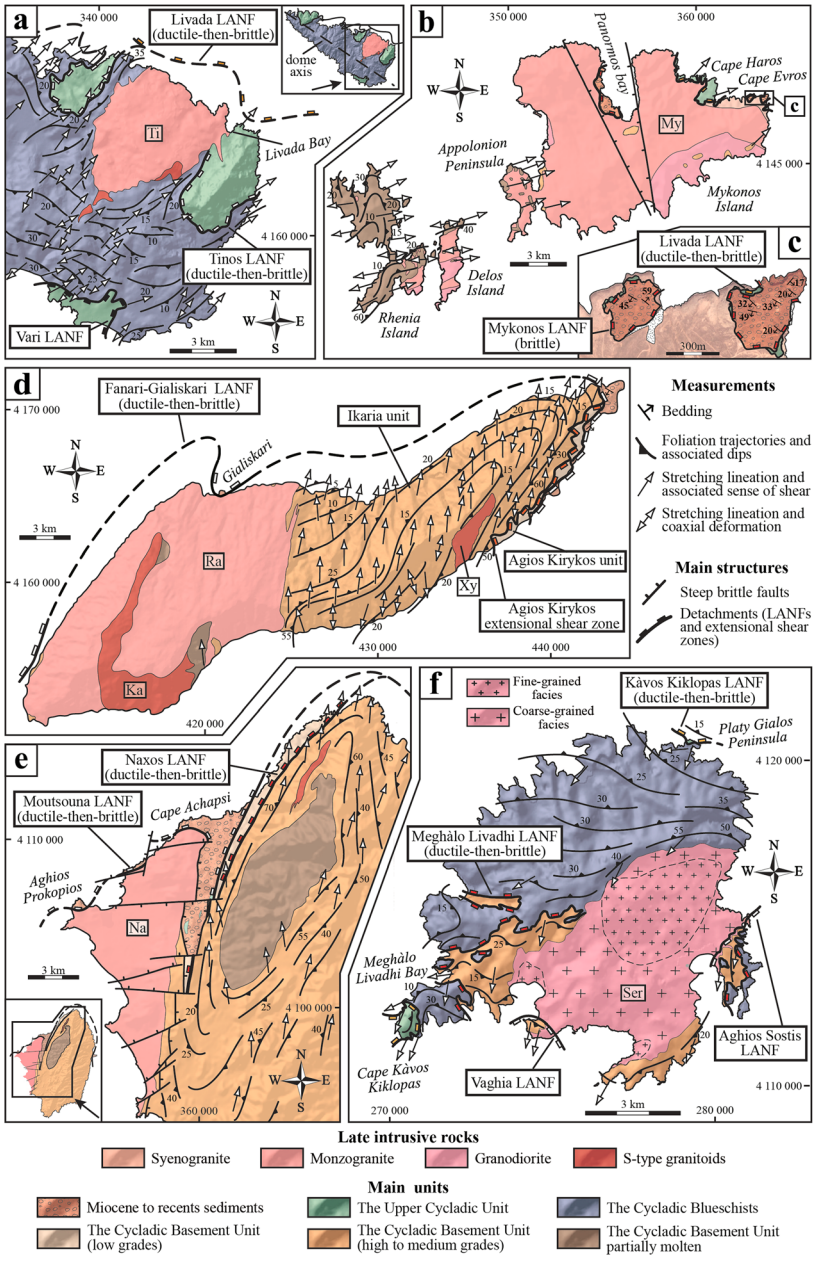

Figure 3. Tectonic maps of the five studied examples of Cycladic metamorphic core complexes and associated intrusions. (a) Tectonic map of the easternmost side of the Tinos metamorphic core complex and associated flanking detachments (location area in the included map inset at upper right showing the NE directed elongated metamorphic dome). Field-based measurements of finite strain markers originate from Melidonis and Triantaphyllis (2003), Famin (2003), Mehl et al. (2005), Jolivet and Patriat (1999), and Jolivet et al. (2010). Ti = Tinos magmatic complex. (b) Tectonic map of the Mykonos-Delos-Rhenia metamorphic core complex and associated flanking detachments. Field-based measurements of finite strain markers originate from Lucas (1999), Lecomte et al. (2010), Denèle et al. (2011), and Menant et al. (2013). My = Mykonos magmatic complex. (c) Detailed tectonic map of Cape Evros area showing the tectonic reworking of the Livada detachment by the brittle-cataclastic Mykonos detachment. (d) Tectonic map of the Ikaria metamorphic core complex and its associated detachment system. Field-based measurements of finite strain markers originate from Photiades (2005), Beaudoin et al. (2015), and Laurent et al. (2015). Ra = Raches monzogranite; Ka = Karkinagrion S-type bimicaceous leucogranite; Xy = Xylosyrtis S-type bimicaceous leucogranite. (e) Tectonic map of the Naxos metamorphic core complex and its associated detachment system. Field-based measurements of finite strain markers originate from Jansen (1973), Gautier et al. (1993), Siebenaller (2008), and Kruckenberg (2009). Na = Naxos monzogranite. (f) Tectonic map of the Serifos metamorphic core complex and its associated detachment system. Field-based measurements of finite strain markers originate from Salemink (1985), Grasemann and Petrakakis (2007), Petrakakis et al. (2010), and Rabillard et al. (2015). Ser = Serifos granodiorite; LANF = low-angle normal fault.

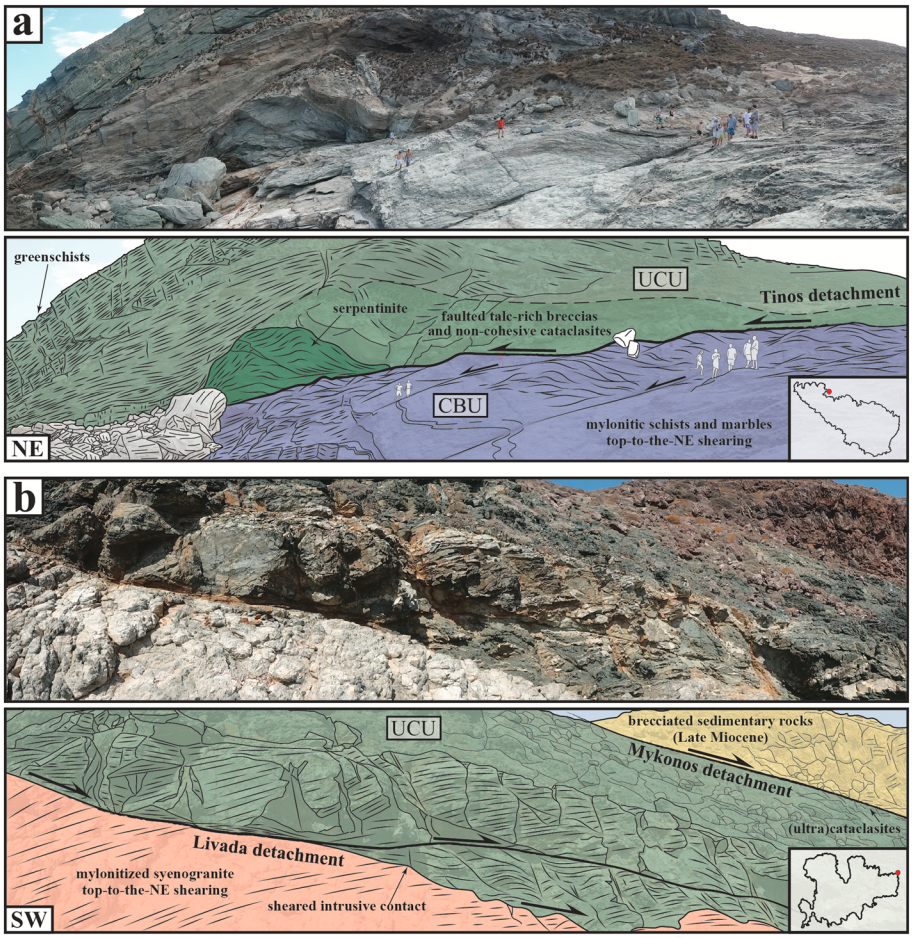

Figure 4. (a) Panoramic view and associated interpretive drawing of the North Cycladic Detachment System running across Tinos Island. View of the ductile-to-brittle Tinos detachment on Planitis Peninsula (location in the included map inset at lower right) where it tectonically juxtaposes the UCU atop the CBU. (b) Panoramic view and associated interpretive drawing of the two closely spaced branches of the North Cycladic Detachment System on Mykonos Island (eastern side of Cape Evros, location in the included map inset at lower right). Bottom: the ductile-to-brittle Livada detachment reworking the intrusive contact between the syenogranite and the UCU. Top: the brittle-cataclastic Mykonos detachment that separates the UCU in the footwall from brecciated sediments in the hanging wall. UCU = Upper Cycladic Unit; CBU = Cycladic Blueschist Unit

Saint Blanquat et al., 2011; Faure et al., 1991; Jolivet et al., 2010). According to Jolivet et al. (2010), this extensional deformation becomes more localized upward and northeastward. Within the lower part of the Upper Unit, ductile shearing was reworked by a system of NW striking, ductile/brittle high-angle normal faults that show a consistent NE-SW direction of extension. Even though no detachment plane has been clearly recognized, this succession of deformation events has been structurally and mechanically correlated with the activity of the Livada detachment that crops out on the nearby island of Mykonos (Figure 3b; Jolivet et al., 2010; Lecomte et al., 2011; Menant et al., 2013). There, the ductile-to-brittle Livada detachment contributed in part to the exhumation of a migmatite-cored dome whose main development is seen on Delos-Rhenia Islands, including a sequence of paragneisses/marbles belonging to the CCB and a 14- to 11-Ma-old magmatic complex slightly younger than the Tinos intrusions (Figures 2 and 3b; Bolhar et al., 2010; Brichau et al., 2008; Faure et al., 1991; Lucas, 1999). This shallow-angle NE dipping detachment operated under a NE directed extensional regime at the contact between the Mykonos intrusion and the UCU (Figures 3c and 4b). Though the apex of the underlying granite was pervasively deformed by a top-to-the-NE simple shear component (for additional information regarding structural records within the Mykonos magmatic complex, see section 4.2), most of the overlying rocks from the UCU do not exhibit any ductile deformation, except directly above the detachment surface where the same northeastward

ductile shearing is locally observed (Cape Haros, Figure 3b; Lecomte et al., 2010; Menant et al., 2013). Similar to the deformation described in Livada Bay (Tinos Island), a late brittle increment occurred along the detachment zone. With a consistent northeastward slip, the top of the footwall together with the UCU was affected by high- and low-angle, east dipping normal faults that crosscut or settle onto the detachment surface (Figure 4b).

Toward the easternmost side of Mykonos Island (Cape Evros, see map location in the Figure 3c), the ductile-to-brittle Livada detachment was dissected by a low-angle cataclastic-brittle structure, that is, the Mykonos detachment (Jolivet et al., 2010; Lecomte et al., 2010). This knife-sharp detachment surface dips 12–15° northeastward and brought in contact Late Miocene synextensional sediments with either the UCU (Cape Evros, Figures 3c and 4b) or the magmatic complex (Panormos Bay and Cape Evros, see Figures 3b and 3c, respectively; Lecomte et al., 2010; Sanchez-Gomez et al., 2002). In both cases, the damaged zone is marked by 1- to 5-m-thick (ultra)cataclasites in the footwall whereas the basal sedimentary sequence displays silicified breccias of up to 10–20 m thick (Lacombe et al., 2013; Lecomte et al., 2010; Menant et al., 2013). These brecciated sediments mainly dip toward the southwest and are reworked by numerous high-angle normal faults rooting onto the detachment surface, thereby describing a block-tilted geometry. Where the detachment surface crops out, it further shows NE oriented striae and corrugations parallel to the measured direction of the stretching lineation in the footwall.

Consequently, it has been largely assumed that strain accommodations and normal sense of displacements along both the Livada and Mykonos detachments would have tectonically controlled the cooling of the granitoid-cored dome, pointing to a relatively fast cooling and a progressive northeastward unroofing between circa 14 and 7 Ma (Figure 2; Altherr et al., 1982; Brichau et al., 2008; Hejl et al., 2002). In the same way on Tinos, available L*T* radiometric ages indicate a nearly concomitant cooling history of the granitoids below the presumed Livada detachment from 15 to 8 Ma (Altherr et al., 1982; Brichau et al., 2007; Hejl et al., 2002).

3.2. Ikaria Island

Located northeast of Mykonos, Ikaria predominantly shows a H*T* metamorphic dome elongated in a NE-SW direction (Figures 1b and 3d; Beaudoin et al., 2015; Martin, 2004; Photiades, 2005). The exhumation history of the metamorphic dome has been especially linked to the tectonic evolution of the northern Cycladic MCCs since structural and thermochronological contributions have emphasized a dominant top-to-the-north shearing component with a progressive strain accommodation through a set of detachments during the Oligo-Miocene (Kumerics et al., 2005; Ring, Will, et al., 2007). Recently, Laurent et al. (2015) and Beaudoin et al. (2015) have refined the tectonic configuration of the detachment system by bringing additional mesostructural observations together with thermometric constraints using Raman spectrometry of carbonaceous material method (Beyssac et al., 2002). According to their interpretation, the final exhumation of the metamorphic dome was controlled by the Agios-Kirykos shear zone and the Fanari-Gialiskari low-angle normal fault (Figure 3d), two closely spaced high-strain zones that respectively acted through time in ductile and ductile-to-brittle fields.

The Agios-Kirykos shear zone has been mapped on the eastern side of the island where it ductilely affected the metamorphic dome and lastly juxtaposed two subunits supposed to represent a part of the CCB, that is, the upper Agios-Kirykos unit and the lower Ikaria unit (Figure 3d). This SE dipping shear zone developed initially with a shallow angle with respect to the compositional layering and was subsequently updomed together with the whole metamorphic sequence (Beaudoin et al., 2015). Based on the distribution of Raman spectrometry of carbonaceous material temperatures acquired over the dome, Beaudoin et al. (2015) further demonstrated that the activity of the Agios-Kirykos shear zone was responsible for a normal sense metamorphic temperature gap. A contrast of deformation style completes the maximum temperature gap between Agios-Kirykos Unit and Ikaria Unit. Deformation is more intense and more ductile within Ikarai Unit. The contact itself does not crop out very well. In the field, structural evidences of the shear zone activity are mostly preserved within the underlying Ikaria unit. Over an approximately 500-m-thick zone, footwall rocks underwent a clear upward strain gradient from low-strain protomylonites observed in the deepest exposed levels of the dome to high-strain mylonites recognized through a band of several tens of meters directly below and above the tectonic contact. The whole strain gradient was also paired with a pervasive top-to-the-north shearing and a synkinematic retrogression into greenschist-facies conditions, while the core of the dome recorded a more

coaxial deformation and retained typical amphibolite-facies associations (600–650 °C for less 600–800 MPa; Kumerics et al., 2005; Martin, 2004). H*T* conditions have also been described in the western part of the island where partially molten gneisses were closely associated with a S-type intrusion (i.e., Karkinagrion granitoid, Figure 3d; Beaudoin et al., 2015; Bolhar et al., 2010; Laurent et al., 2015).

Toward the easternmost side of the island, the metamorphic dome is tectonically topped by the Fanari-Gialiskari detachment (Figure 3d; Beaudoin et al., 2015; Laurent et al., 2015). This south to SE dipping detachment cuts down through the Agios-Kirykos shear zone and structurally puts in direct contact Late Miocene to Early Pliocene syntectonic sediments on either Agios-Kirykos unit (Figure 5a) or Ikaria unit. Associated with top-to-the-north or top-to-the-NE kinematics, extensional shearing in the footwall evolves toward the detachment fault plane from medium-grade mylonites to low-grade ultramylonites. Unlike the Agios-Kirykos shear zone, the Fanari-Gialiskari detachment zone displays evidences of subsequent displacements in the brittle field. The highly sheared rocks were partially reworked by cataclasites and fault rocks within a thin section of a few meters below the corrugated detachment fault surface, carrying itself large-scale displacement features in brittle conditions. As suggested by paleostress analyses, development of late brittle structures was persistently controlled by an overall NE oriented extension (Beaudoin et al., 2015; Kumerics et al., 2005). On the basis of structural and geometrical similarities, the detachment has been furthermore extended as far as the northeastern part of Ikaria toward the Gialiskari Peninsula (Figure 3b) where syntectonic sediments rest directly above the I-type Raches intrusion (Figure 5b, further details in section 4.3; Beaudoin et al., 2015; Laurent et al., 2015).

On Ikaria, accurate radiometric time constraints for the extensional shearing initiation along both detachments and their relative timing are currently poorly known. However, the exhumation history of the metamorphic dome is roughly constrained by the approximately 25- to 17-Ma ages retrieved from amphibolite-facies sheared rocks (Altherr et al., 1982) and the 11.5- to 9-Ma ages acquired on fabric-forming micas from the uppermost levels of the dome (Figure 2; Altherr et al., 1982; Kumerics et al., 2005). Additionally, timing of the H*T* thermal event was constrained by recent (U-Th)/Pb analyses on monazite from the leucosome parts of migmatitic gneisses, thus yielding a 15.7 ± 0.2-Ma age (Figure 2; Beaudoin et al., 2015). Beaudoin et al. (2015) tentatively concluded that extensional shearing and strain localization along the Agios-Kirykos shear zone might have started at or even before this H*T* thermal event, later followed by the emplacement of two S-type granitoids between approximately 15 and 14 Ma (i.e., the Xylosyrtis and Karkinagrion intrusions) and the 14-Ma-old I-type Raches granitoid (Figure 2; Bolhar et al., 2010). On the basis of available L*T* geochronological data, both the intrusions and the host metamorphic sequence were eventually subjected to a joint cooling episode with reported ages from ~10 to as young as ~4 Ma, together with an apparent northward and upward unroofing in correspondence with the observed top-to-the-north extensional shearing (Altherr et al., 1982; Kumerics et al., 2005).

3.3. Naxos Island

Naxos Island lies within the central part of the Cyclades where the development of large-scale MCCs was governed by an overall north directed extension and a top-to-the-north shearing through the NPDS (Figure 1b and 1c; Bargnesi et al., 2013; Brichau et al., 2006; Gautier et al., 1993). On Naxos, the late exhumation stage was historically interpreted as stemming from progressive strain localization along a single crustal-scale detachment (i.e., the Moutsouna detachment, Figure 3e; Buick, 1991a, 1991b; Lister et al., 1984; Urai et al., 1990). This localizing event partly brought toward upper crustal levels a H*T* metamorphic dome dominated by a migmatitic gneiss core preserving Variscan protolithic ages of the original CCB (Andriessen et al., 1987; Jolivet, Rimmelé, et al., 2004; Vanderhaeghe, 2004) and a cover series mostly made of marbles and metapelites that locally retains the former Eocene H*P*-L*T* metamorphic event (Andriessen et al., 1979; Avigad, 1998; Peillod et al., 2017; Wijbrans & McDougall, 1986, 1988). More recently, field investigations and resulting tectonic maps have shown a more complex tectonic architecture with two closely spaced branches of the NPDS (Kruckenberg, 2009; Siebenaller, 2008; Siebenaller et al., 2013). According to the updated geological map (Figure 3e), the detachment system includes the previously mapped Moutsouna detachment and the Naxos detachment. During their activity, both detachments were associated with similar top-to-the-north displacements and a comparable tectonic evolution from ductile-to-brittle conditions. The detachment system was further folded together with foliations of the migmatitic dome, undulating in large-scale synforms and antiforms whose axes trend parallel to the north directed stretching lineation (Figure 3e; Avigad et al., 2001; Buick, 1991a; Kruckenberg et al., 2011).

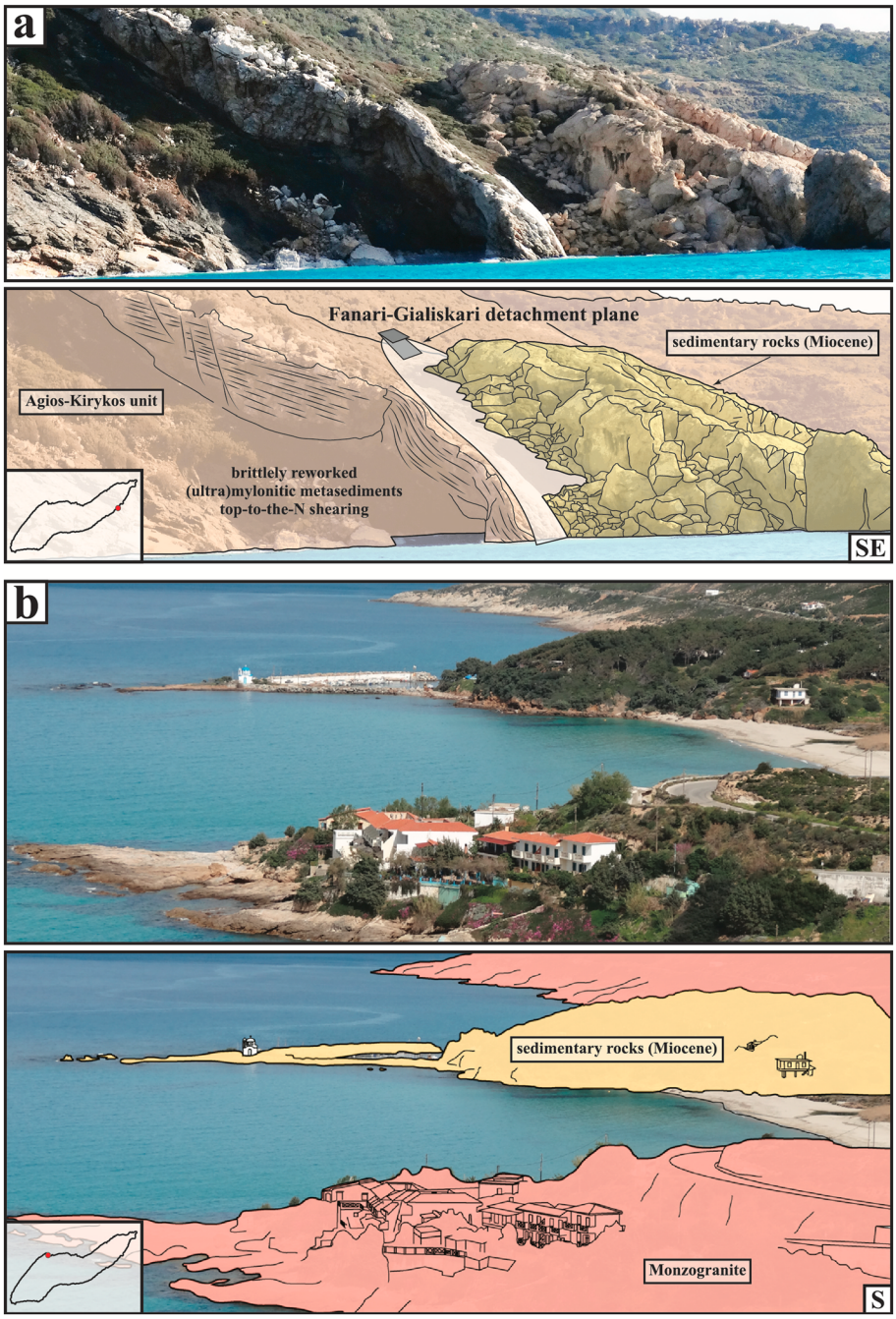

Figure 5. Panoramic views and associated interpretive drawings of the ductile-to-brittle Fanari-Gialiskari detachment belonging to the North Cycladic Detachment System on Ikaria Island. (a) View of the south dipping detachment surface toward the southeastern coast of the Island (location in the included map inset at lower left) where it tectonically separates the underlying Agios-Kirykos unit from brecciated and faulted sedimentary rocks. (b) View of the same detachment at Gialiskari (location in the included map inset at lower left) where it dips to the north and puts in direct contact the syn-tectonic sedimentary basin on the Raches intrusive body.

Across the entire exposed metamorphic dome, both flanking detachment fault planes discontinuously crop out due to the late brittle reworking of kilometric-scale steep, normal to transtensional faults (Figure 3e; Gautier et al., 1993; Jansen, 1973; Siebenaller, 2008; Vanderhaeghe, Hibsch, Siebenaller, Duchêne, Kruckenberg, et al., 2007). The Naxos detachment fault can only be traced at the northwestern flank of the migmatitic dome where it tectonically dismembered the presumed CCB. Below this steeply NW dipping

detachment, footwall rocks recorded an upward and northwestward noncoaxial shear gradient through a thick section of several hundred meters (Siebenaller, 2008). Coeval with a retrograde metamorphism, mesoscopic and microscopic criteria thus support a spatial evolution of deformation from amphibolite-facies protomylonites and mylonites surrounding the migmatite-cored dome to greenschist-facies ultramylonites when approaching the detachment surface (Kruckenberg et al., 2011; Siebenaller, 2008). Throughout the detachment zone, late brittle-cataclastic increments have been exclusively observed close to the tectonic contact with several meter thick cataclasites that reworked ultramylonites in the footwall, while low-grade metamorphic rocks from the hanging wall were intensely brecciated over a thin section of a few meters (Siebenaller, 2008).

Structurally higher up, the low-grade metamorphic sequence was, in turn, tectonically unroofed by the Moutsouna detachment (Figure 3e). This detachment displays a sharp fault surface and extension-parallel corrugations with wavelengths ranging from the meter scale to several hundred meters (Gautier et al., 1993), above which lies a syntectonic basin primarily filled with Miocene deposits and containing remnants of ophiolitic rocks issued from the UCU (Figure 3e; Angelier et al., 1978; Jansen, 1973; Kuhlemann et al., 2004). The detachment zone has been likewise laterally extended on the eastern flank of the dome where it dips moderately eastward (Figure 6a, location in the map inset at lower right).

There, the activity of the present-day north striking detachment zone was clearly associated with an intense top-to-the-north mylonitization of footwall rocks depicted by an upward shear strain gradient coupled with a retrograde metamorphism into greenschist-facies conditions (Cao et al., 2013; Gautier et al., 1993; Vanderhaeghe, Hibsch, Siebenaller, Duchêne, de St Blanquat, et al., 2007). The penetrative amphibolite-facies deformation and related concentric H*T* metamorphic isograds recorded in the lowermost parts of the dome were upwardly intersected and erased by these synkinematic greenschist-facies recrystallizations (Gautier et al., 1993). Besides, superimposition of ductile structures by brittle ones has been locally observed underneath the fault plane where the strongly sheared rocks were reworked by tectonic microbreccias, a dense network of fractures and variously striking normal faults (Cao et al., 2013; Gautier et al., 1993; John & Howard, 1995). Several high-angle normal faults have also been identified within the sedimentary basin, rooting or cutting through the detachment surface (Figure 6a). This ductile-then-brittle event has been approximately recorded through a thick zone of a few hundred meters, suggesting that extension below the Moutsouna detachment was accommodated in more localized horizons than underneath the Naxos detachment. Considering the above tectonometamorphic features, the development of the Moutsouna detachment arguably postdated the activity of the Naxos detachment and ultimately dissected through it, most likely farther offshore north of the island (Figure 3e).

On Naxos Island, timing for ductile deformation is provided by a large set of thermochronological tools (Figure 2) that indicate a ~25- to 8-Ma-old greenschist-facies metamorphism within the lower-grade rocks (Andriessen, 1991; Andriessen et al., 1979; Cao et al., 2017; Wijbrans & McDougall, 1986, 1988) and a peak of H*T* between 21 and 14 Ma within high-grade amphibolite-facies rocks (Andriessen, 1991; Martin et al., 2006; Wijbrans & McDougall, 1986, 1988) where the anatectic episode was consistently dated between 21 and 17 Ma (Keay et al., 2001). Consequently, it was hypothesized that extensional shearing onset and strain localization would have preceded or coincided with the H*T* thermal event (Buick & Holland, 1989), but paroxysm of strain accommodation along the detachment system would have been achieved between 17 and 8 Ma (Brichau et al., 2006; John & Howard, 1995). While shear strain was already initiated, both S- and I-type granitoids intruded the metamorphic dome at circa 15–13 and 13–11 Ma, respectively (Figure 2 and 3e; Bolhar et al., 2010; Keay et al., 2001). Along with the whole metamorphic pile, the I-type granitoid cooled into the upper crust over a rather short time span of ~4 Ma after its emplacement (Figure 2; Brichau et al., 2006; Keay, 1998; Pe-Piper et al., 1997; Seward et al., 2009; Wijbrans & McDougall, 1988). Low-temperature geochronological investigations performed within this granitoid further yielded an apparent northward rejuvenation of cooling ages, consistent with the top-to-the-north tectonic unroofing thought to be induced by the activity of the Moutsouna detachment exposed at the northern rim of the intrusion (Figures 3e and 6b; see section 4.4 for further details; Brichau et al., 2006; Seward et al., 2009).

3.4. Serifos Island

Serifos Island is part of the western Cyclades where a series of metamorphic domes were exhumed below the WCDS under an overall SW directed extensional regime (Figures 1b and 1c; Grasemann et al., 2012; Iglseder

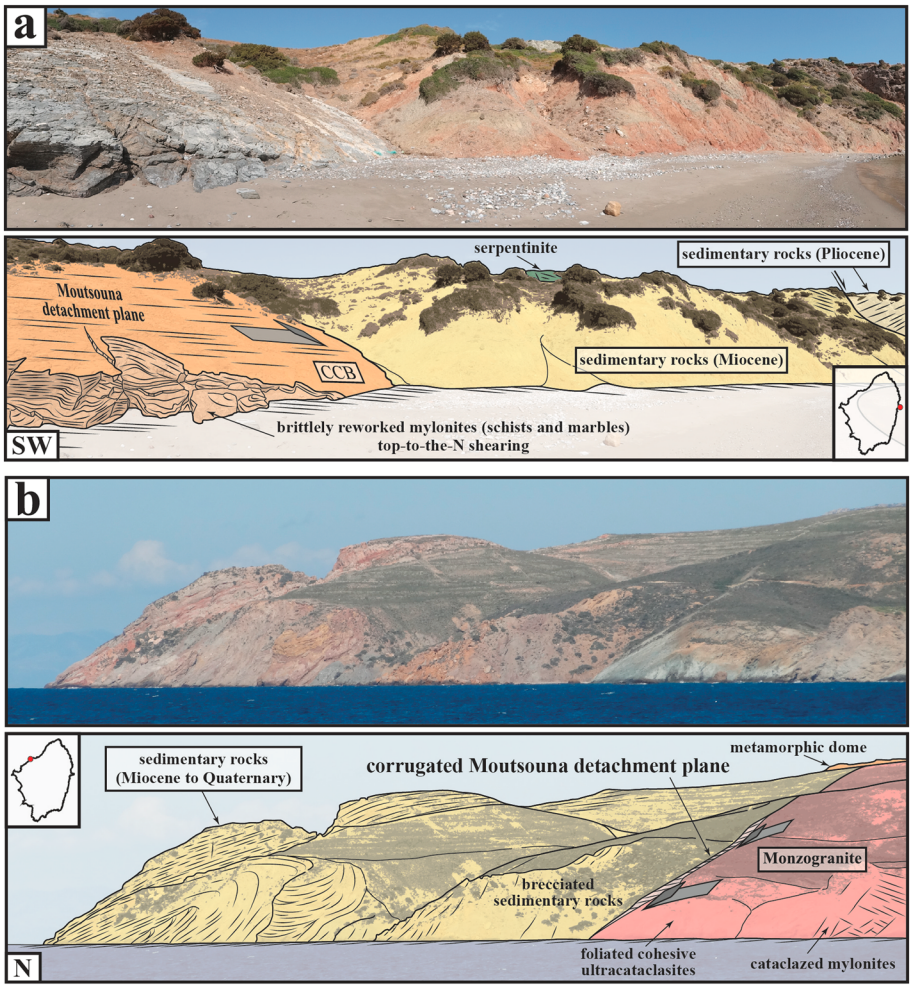

Figure 6. Panoramic views and associated interpretive drawings of the ductile-to-brittle Moutsouna detachment belonging to the Naxos-Paros Detachment System on Naxos Island. (a) View of the east dipping detachment plane toward the easternmost part of the island (Moutsouna peninsula, location in the included map inset at lower right) where brittlely reworked mylonites from the CCB tectonically underlie Miocene sedimentary deposits and relics of ophiolitic rocks (serpentinites) from the UCU. (b) View of the corrugated detachment surface at Cape Achapsi (location in the included map inset at upper left) where the brecciated sedimentary rocks rest directly above the (ultra)cataclazed monzogranite. CCB = Cycladic Continental Basement; UCU = Upper Cycladic Unit.

et al., 2011). Among the western Cycladic domes, Serifos Island offers the most complete structural section with a metamorphic dome incised by the lower Meghàlo Livadhi detachment and the upper Kàvos Kiklopas detachment, two branches of the WCDS that have tectonically put in direct contact the CBU upon the CCB and the UCU upon the CBU, respectively (Figures 3f, 7a, and 7b; Grasemann & Petrakakis, 2007; Grasemann et al., 2012; Rabillard et al., 2015). Along a cross section parallel to the NE-SW stretching lineation, the detachment system has been arched upward with SW dipping planes on the southwestern tip (Cape Kàvos Kiklopas and Meghàlo Livadhi Bay) and NE dipping surfaces in the northeast (Platy Gialos Peninsula). Previous structural field investigations have further shown that both detachments shared a similar tectonic evolution during their development involving a top-to-the-SW, ductile-to-brittle extensional deformation (Grasemann & Petrakakis, 2007; Grasemann & Tschegg, 2012).

Associated with an exhumation-related retrogressive metamorphism under typical greenschist-facies conditions, the top-to-the-SW ductile deformation was extremely localized in the footwall of both detachment fault planes (Dabrowski & Grasemann, 2014; Grasemann & Tschegg, 2012), leaving an earlier well-preserved E-W to ENE-WSW trending stretching lineation in large parts of the dome attributed to an Eocene (high

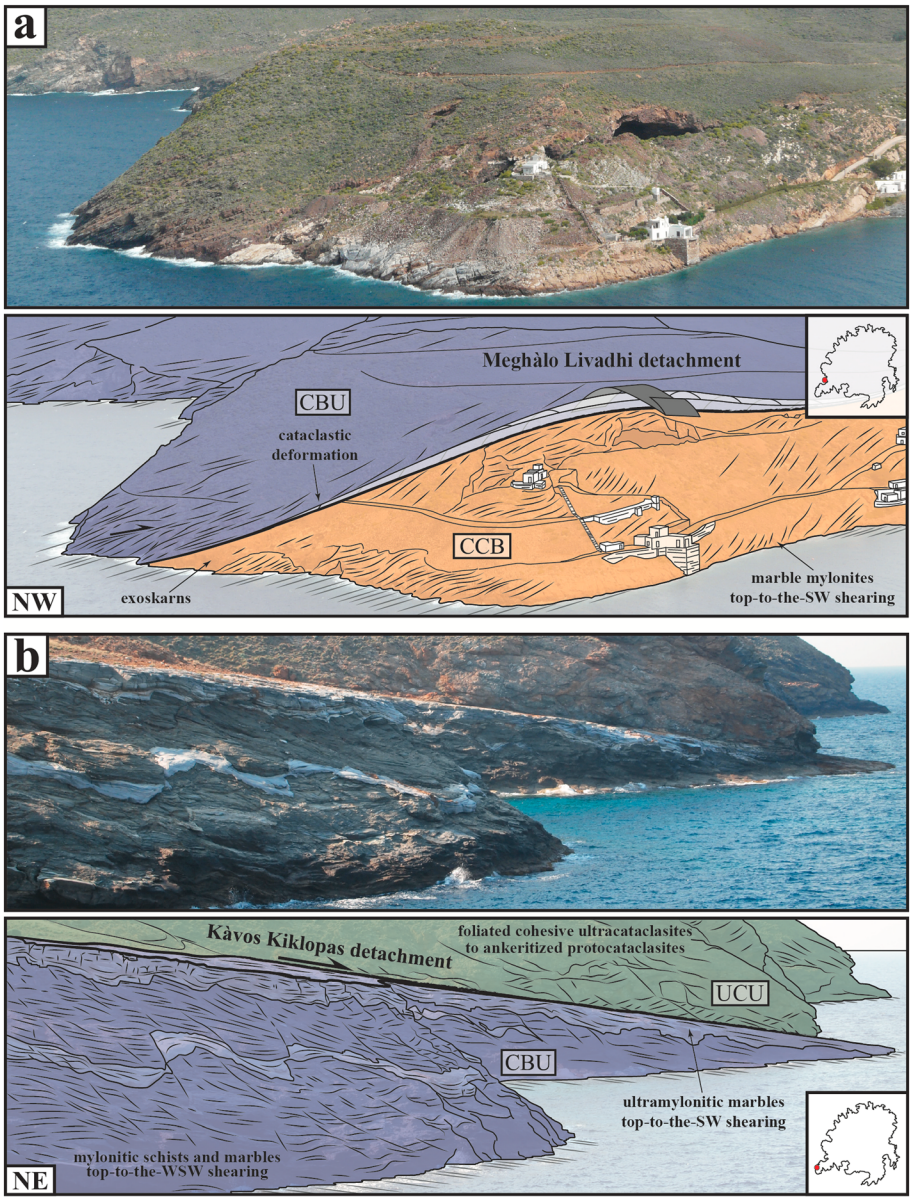

Figure 7. Panoramic views and associated interpretive drawings of the West Cycladic Detachment System on Serifos Island. (a) View of the lowermost ductile-to-brittle Meghàlo Livadhi detachment (location in the included map inset at upper right); it separates the CCB (marble mylonites) in the footwall from the CBU (cataclastic greenschists and amphibolites) in the hanging wall. (b) View of the uppermost ductile-to-brittle Kàvos Kiklopas detachment (location in the included map inset at lower right) juxtaposing the UCU above the CBU. CCB = Cycladic Continental Basement; CBU = Cycladic Blueschist Unit; UCU = Upper Cycladic Unit.

pressure?) metamorphic episode (Figure 3f; Cossette et al., 2015; Schneider et al., 2011). Beneath the Meghàlo Livadhi detachment fault surface, extensional shearing was heavily concentrated at the top of the CCB where metamorphic rocks were mylonitized under an upward strain gradient over several tens of meters in thickness and subsequently intersected by sets of high- and low-angle normal faults (Grasemann & Petrakakis, 2007; Grasemann & Tschegg, 2012). By contrast, most of the overlying rocks from the CBU were subjected to an intense cataclastic-brittle deformation featured by a level of metasomatized breccias and cataclasites not thicker than a few tens of meters (Figure 7a). Although ductile deformation appears indistinguishable at the base of the CBU, top-to-the-SW meter-scale shear bands have been locally described somewhat higher up in the metamorphic pile, showing a probable downward reworking of ductile structures by brittle ones when approaching the detachment surface. Comparatively, the

southwestward shearing just below the Kàvos Kiklopas detachment was restricted within a much thinner section of about 2 m along which the apical rocks of the CBU were ultramylonitized (Figure 7b; Grasemann & Petrakakis, 2007; Rabillard et al., 2015). Basal rocks of the structurally overlying UCU then recorded a preeminent cataclastic deformation through an apparent thickness of several tens of meters, moving up from a detachment gouge and foliated/folded cohesive ultracataclasites at the base to ankeritized protocataclasites toward upper levels (Figure 7b). Where the detachment surface crops out, it clearly bears slickenline lineations compatible with the shear sense deduced from the underlying CBU. Finally, metamorphic rocks from both the CBU and the UCU were cut by well-defined NW striking, conjugate low- and high-angle normal faults that display consistent SW oriented offsets.

According to published geochronological data, age constraints on each detachment activity remain unclear as the retrograde greenschist-facies metamorphic recrystallization was almost completely erased by amphibolite-facies parageneses, plausibly induced by the I-type igneous event that intruded the metamorphic dome (Figure 3f) or by a regional H*T* event (Grasemann et al., 2012; Iglseder et al., 2009). However, available thermochronological data yielded syngreenschist-facies mylonitization ages below the Meghàlo Livadhi detachment between 15 and 11 Ma, while the main Serifos granitoid intruded the CBU and pierced the deeper Meghàlo Livadhi detachment between 11.6 and 9.5 Ma (Figure 2; Iglseder et al., 2009). It is, however, likely that extensional tectonics started earlier than 15 Ma in this region, probably as soon as the early Miocene (Grasemann et al., 2012). Low-temperature ages lastly indicate a fast cooling history of both the metamorphic dome and the intrusion below the Kàvos Kiklopas detachment over a period spanning from ~9 to ~4 Ma (Altherr et al., 1982; Brichau et al., 2010; Grasemann et al., 2012; Hejl et al., 2002).

To summarize a few major points from the above section, it appears that the Oligo-Miocene, extension-related exhumation processes of the targeted Cycladic metamorphic domes occurred consistently below multiple and closely spaced high-strain zones that diversely evolved under ductile (i.e., the Agios-Kirykos shear zone), ductile-then-brittle (i.e., the Tinos, Livada, Fanari-Gialiskari, Naxos, Moutsouna, Meghàlo Livadhi, and Kàvos Kiklopas low-angle normal faults), or purely brittle conditions (i.e., the Mykonos low-angle normal fault). At the scale of a single metamorphic dome, the flanking detachments developed through time with a quite similar sense of shear and/or slip, and it appears that the most deeply exposed branches have been cut downward by more surficial ones. This was recently confirmed in a recent paper on Serifos by Seman et al. (2017), who presented detrital zircon U-Pb analyses indicating that the Kavos Kyklopas detachment certainly cuts down section in the CBU toward the SW. In parallel, metamorphic domes were intruded by I- and S-type granitoids while exhumation and corresponding greenschist- to amphibolite-facies retrograde metamorphism seemed to be already initiated (Figure 2). First-order geometrical aspects further show that (1) some granitoid roofs obviously intruded hanging wall rocks of preexisting detachments (i.e., the Tinos and Serifos intrusions, see tectonic maps in Figure 3) and (2) all of them structurally lie beneath more surficial detachment fault planes.

4. Petrostructural Records Within the Cycladic Granitoids

The present section includes both a brief overview of the igneous rock types exposed in the targeted Cycladic MCCs and a more comprehensive description devoted to the state of finite strain fossilized inside each magmatic complex. With the objective of illustrating lateral shear gradients over both granitoids of Mykonos and Ikaria, Denèle et al. (2011) and Laurent et al. (2015), respectively, elaborated a qualitative scale of strain intensity by defining a succession of deformation grades. By integrating the preexisting data together with our own structural observations, a similar approach with distinctive scales of fabric intensity has been applied across the remaining granitoids of Tinos, Naxos, and Serifos. The resulting maps of large-scale patterns of deformation (see Figure 8) are compiled with field-based measurements of finite strain markers and, if appropriate, combined with magnetic fabrics issued from additional laboratory investigations using the anisotropy of magnetic susceptibility (AMS method, for reviews and basic principles see, e.g., Borradaile & Henry, 1997; Borradaile & Jackson, 2010). Note that though transitions from one grade to another appear gradual in the field, those on the maps have been drawn abruptly for the sake of simplification.

4.1. The Tinos Magmatic Complex

Intrusive within the northeastern part of the metamorphic dome, the Tinos magmatic complex encompasses an I-type biotite-hornblende monzogranite circumscribed by two smaller S-type garnet-bearing

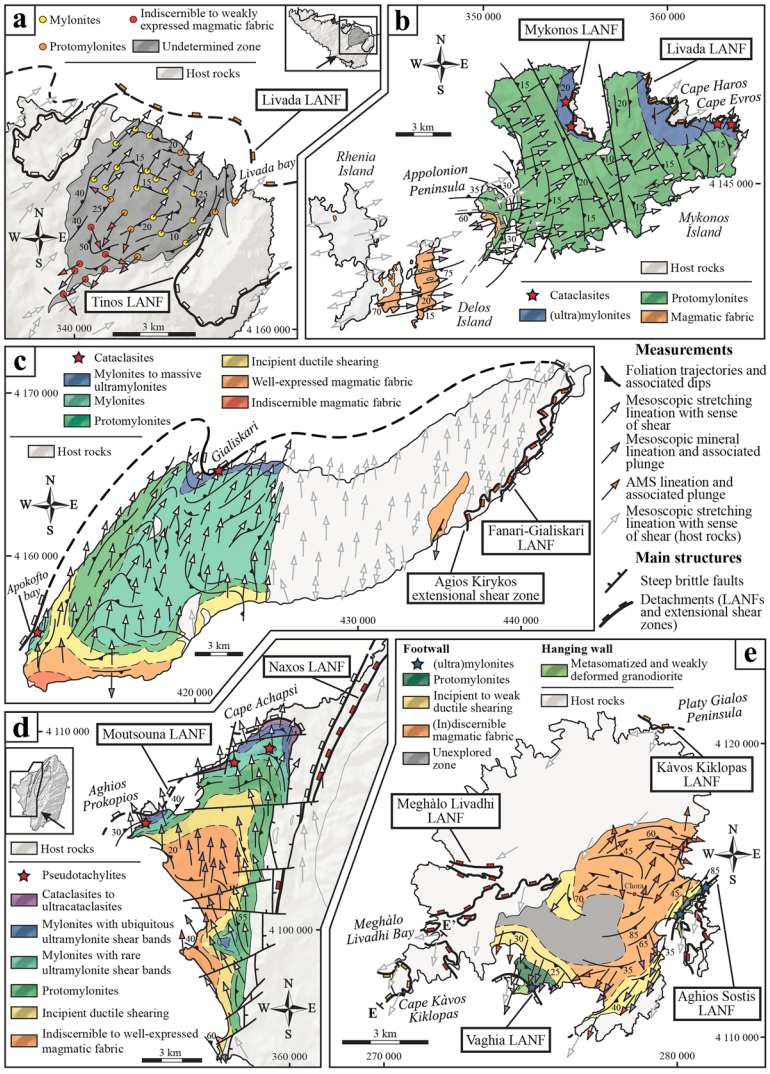

Figure 8. Tectonic maps of the five field examples of Cycladic metamorphic core complexes and associate detachments studied in this paper with maps of strain intensity. (a) Tectonic map of the Tinos magmatic complex incorporating a distribution map of the strain intensity qualitatively built from microscopic and macroscopic observations on which it has been superposed finite strain markers (interpolated foliation trajectories, mineral and stretching lineations) collected from field-based and AMS measurements. For comparison, stretching lineations recorded over the adjacent metamorphic domes are also redrawn (bleached arrows); data acquired by Habert (2004), Jolivet et al. (2010), and de Saint Blanquat et al. (2011). (b) Tectonic map of the Mykonos magmatic complex incorporating a distribution map of the strain intensity qualitatively built from microscopic and macroscopic observations on which it has been superposed finite strain markers (interpolated foliation trajectories, mineral and stretching lineations) collected from field-based measurements. For comparison, stretching lineations recorded over the adjacent metamorphic domes are also redrawn (bleached arrows); data are acquired by Lucas (1999) and Denèle et al. (2011). (c) Tectonic map of the Ikaria magmatic complex incorporating a distribution map of the strain intensity qualitatively built from microscopic and macroscopic observations on which it has been superposed finite strain markers (interpolated foliation trajectories and mineral and stretching lineations) collected from field-based measurements. For comparison, stretching lineations recorded over the adjacent metamorphic domes are also redrawn (bleached arrows); data are acquired by Kokkalas and Aydin (2013) and Laurent et al. (2015). (d) Tectonic map of the Naxos monzogranite incorporating a distribution map of the strain intensity qualitatively built from microscopic and macroscopic observations on which it has been superposed finite strain markers (interpolated foliation trajectories, mineral and stretching lineations) collected from field-based and AMS measurements. For comparison, stretching lineations recorded over the adjacent metamorphic domes are also redrawn (bleached arrows). (e) Tectonic map of the Serifos granodiorite incorporating a distribution map of the strain intensity qualitatively built from microscopic and macroscopic observations on which it has been superposed finite strain markers (interpolated foliation trajectories, mineral and stretching lineations) collected from field-based and AMS measurements. For comparison, stretching lineations recorded over the adjacent metamorphic domes are also redrawn (bleached arrows); data acquired by Rabillard et al. (2015). AMS = anisotropy of magnetic susceptibility; LANF = low-angle normal fault.

leucogranites (Figure 3a; Altherr et al., 1982; Altherr & Siebel, 2002; Bröcker & Franz, 1998; Melidonis, 1980). Besides the existing broad geochemical and compositional discrepancies between the two rock types, the large-scale monzogranite additionally distinguishes itself from leucogranites through its internal petrotextural heterogeneities. By means of mesoscopic and microscopic observations, Habert (2004) emphasized within the monzogranite a rather concentric textural zoning with an inward evolution from a fine- to a coarser-grained facies. This texturally zoned body further encloses sporadic petrological heterogeneities exemplified in the field either by disseminated vestiges of nonamalgamated magmatic intrusions, such as isolated microgranitoid enclaves and synplutonic dikes, or by compositional bandings underlined by biotite-enriched layers (Altherr & Siebel, 2002; Habert, 2004).

From an architectural point of view, the partially exposed magmatic complex has been defined as a semielliptical, pluton-shaped body dominated by a NE directed long axis (Figure 8a; Brichau et al., 2007; de Saint Blanquat et al., 2011; Habert, 2004). Such a 3-D finite configuration, inferred from foliation traces, has been regarded as the consequence of a pervasive top-to-the-NE ductile deformation that affected the northeastern two thirds of the monzogranite. Conversely, plutonic rocks from the southwestern edge have preserved magmatic textures with mesoscopically indiscernible or weakly expressed mineral fabrics, devoid of any superposed plastic deformation or recrystallization. Nonetheless, by combining contributions of field measurements and AMS results, it has been evidenced an overall prolate fabric marked by a bimodal direction of mineral and magnetic lineations with a predominant northeast trend and a subsidiary perpendicular family exclusively detected by AMS signal (Habert, 2004, Figure 13). These lineations are carried by foliations roughly parallel to those from wall rocks (de Saint Blanquat et al., 2011; Habert, 2004).

Farther to the northeast, intrusive rocks were progressively affected by a solid-state shear strain gradient with a northeastward continuum from low-strain to high-strain mylonites (Figure 8a). The protomylonitic grade has been also recognized in the northeastern part of the monzogranite (Livada Bay) where the pluton rim and closely associated synplutonic sills intruding the UCU were damaged by a nonpervasive top-to-the-NE shearing materialized by discrete NE dipping shear bands and shallow-angle and steeper normal faults (Brichau et al., 2007; de Saint Blanquat et al., 2011; Jolivet et al., 2010). Mylonitic bands can also be observed locally in this region (K. Soukis, personal communication, 2016) otherwise dominated by protomylonitic deformation. Most of intensely sheared rocks have been found in the central and western domains of the monzogranite where the highest topographic zones are tectonically capped by mylonitic rocks. Mylonites bear subhorizontal tectonic foliations, well-grouped NE trending stretching lineations and unchanging top-to-the-NE kinematics. Locally, the mylonitic fabric was subsequently reworked by high-angle normal ductile-then brittle shear zones, breccias, cataclasites or even crosscut by pseudotachylytes (Brichau et al., 2007; Habert, 2004; Kokkalas & Aydin, 2013). This successive sequence of ductile-then-brittle fabrics implies a proximal influence of a localized major structure at an upper level, supposed to be connected with the activity of the detachment (de Saint Blanquat et al., 2011; Jolivet et al., 2010).

4.2. The Mykonos-Delos-Rhenia Magmatic Complex

On the Mykonos-Delos-Rhenia archipelago, the Miocene intrusive magmatism stands out from the other Cycladic plutonic events by a greater range of petrological rock types (Figure 3b). From the more differentiated ones to the mafic ones, four petrographic types have been recognized: (1) a syenogranite localized below the detachment system near Cape Evros (Figure 3c) where the intrusive contact with the UCU has been locally described (Figure 4b); (2) a biotite-hornblende monzogranite enclosing rare mafic enclaves but rather rich in xenoliths and septa from the migmatitic dome; and (3) a biotite-hornblende granodiorite with abundant schlierens, isolated enclaves and monogenic/polygenic swarms of enclaves and (4) a pyroxene porphyric granodiorite (Denèle et al., 2011; Lecomte et al., 2010; Lucas, 1999; Pe-Piper et al., 2002). These granitoids are primarily delimited by outcrop-scale sharp transitions and form sheet-like intrusions at the scale of the magmatic complex (Denèle et al., 2011; Lucas, 1999). The aforementioned surveys reported NE-SW striking, steeply to moderately dipping magmatic sheets on Delos-Rhenia Islands and gentler NE dipping petrological contacts over Mykonos Island (Figure 8b). These observations outline a flat-lying sheeted complex in which the more mafic intrusions constitute the deepest portions.

Via key microstructural and macrostructural investigations, a continuous deformation history from magmatic to solid-state ductile/brittle conditions under an overall NE directed strain component has been identified inside the plurikilometric-scale magmatic complex (Denèle et al., 2011; Faure et al., 1991; Lucas, 1999). The

early magmatic or subsolidus deformational event has been especially preserved on Delos-Rhenia Islands, close to the migmatitic dome and therefore far away from the detachment system (Figure 8b). Apart from some near-solidus microstructures revealed by the fracturing of feldspar phenocrysts healed with magmatic minerals (see Bouchez et al., 1992, for melt-present fracturing clues), intrusive rocks display typical magmatic microtextures devoid of significant solid-state imprints (Denèle et al., 2011; Lucas, 1999). In the field, previous works further highlighted a mainly prolate magmatic fabric with a steady ENE trending, shallowly east plunging mineral lineation carried by weakly expressed NE striking foliations subparallel to petrological contacts (Figure 8b; Denèle et al., 2011; Faure et al., 1991; Lucas, 1999). On Mykonos, even if a broad zone of the magmatic complex recorded a noncoaxial extensional shearing, the synmagmatic deformation can still be discernible in a geographically limited area around the Appolonion Peninsula (Figure 8b). Thence, the incompletely superimposed magmatic fabric progressively evolves from prolate to weakly oblate. In map view, the above described NE striking, steeply dipping foliation trajectories drastically deflect and draw a subelliptical architecture, elongated parallel to the persistent ENE trending mineral lineation (Denèle et al., 2011; Faure et al., 1991; Lucas, 1999).

The magmatic complex displays northeastward a diffuse finite ductile strain gradient from protomylonitic to (ultra)mylonitic grades (Figure 8b). The transition from the magmatic domain to the protomylonitic one has been thereby underlined near Appolonion Peninsula through relics of high- to medium-temperature solid-state microstructures, as well as incipient shear localization of nonpervasive, gently NE dipping shear bands that homogeneously indicate a top-to-the-ENE sense of shear (Denèle et al., 2011; Lucas, 1999). These millimeter-wide, normal sense shear bands become increasingly denser and thicker northeastward up to grow into a mylonitic zone just below the detachment system. Here a several tens of meter thick section displays mylonitized rocks characterized by shallow NE dipping tectonic foliations, a slightly deviated NE trending stretching lineation and various kinematic criteria compatible with a top-to-the-NE sense of shear (Figure 8b; Avigad et al., 1998; Denèle et al., 2011; Faure et al., 1991; Lecomte et al., 2010; Lee & Lister, 1992; Menant et al., 2013).

In line with the upward and northeastward strain gradient, the most intensely deformed rocks have been documented within the uppermost decametric section underneath the detachment surfaces and especially below the Livada detachment plane where it crops out several centimeter- to meter-wide ultramylonite bands (Jolivet et al., 2010; Lecomte et al., 2010; Menant et al., 2013). These ultramylonitic shear bands, together with the penetrative mylonitic foliation and the locally observed intrusive contact, were asymmetrically folded under a similar NE directed simple shearing (Figure 4b). The deformational history ended into semibrittle to brittle conditions. The last incremental motions can be chiefly sighted through all the northeastern border of the intrusion. The strongly sheared intrusive body, along with its related train of sills and dikes, was reworked by synthetic and antithetic Riedel faults or by the above reported massive (ultra)cataclastic deformation linked to the Mykonos detachment activity (see section 3.1; Lacombe et al., 2013; Lecomte et al., 2010; Menant et al., 2013).

4.3. The Ikaria Magmatic Complex

On Ikaria, magmatic products were predominantly accumulated into the western half of the dome where the I-type Raches intrusion was spatially emplaced after the S-type Karkinagrion intrusion that is associated with migmatites in the southern part of the island (Figure 3d), two plurikilometric-scale bodies respectively affiliated to a biotite-hornblende monzogranite (Altherr et al., 1982; Altherr & Siebel, 2002) and a two-micas leucogranite (Bolhar et al., 2010; Ring, 2007). These two closely associated granitoids embody together a nested magmatic system wherein the large-scale I-type monzogranite hosts a composite network of synplutonic dikes that intrude the MCC (Laurent et al., 2015). Synplutonic dikes have been widely recognized in outer zones of the magmatic system, in particular, all the way through the eastern margin where the folded intrusive contact with the metamorphic sequence can be followed over approximately 10 km in a north-south direction (Beaudoin et al., 2015; Laurent et al., 2015). The contact between the Raches granite and the MCC has complex geometry as it has been sheared and folded with axes parallel to the regional shearing direction (Laurent et al., 2015). Farther east, the H*T* metamorphic dome was also intruded by the small-scale Xylosyrtis granitoid (Figure 3d), another S-type two-micas leucogranite surrounded by a dense array of pegmatitic and aplitic dikes (Altherr et al., 1982; Hezel et al., 2011; Kumerics et al., 2005; Photiades, 2005). Though it was intrusive within the upper metamorphic pile of the Ikaria unit close to the detachment system, the

satellite Xylosyrtis leucogranite appears ductilely less deformed but shows a clear stretching parallel to the regional shearing direction. Mainly a mineral fabric, probably acquired under a magmatic state, has been distinguished and defined by faintly pronounced SE dipping foliations and NE trending lineations (Figure 8c; Kokkalas & Aydin, 2013).

Conversely, nearly all of the Raches-Karkinagrion magmatic system experienced a significant solid-state deformation under ductile and brittle fields, partially or completely obliterating the primary magmatic texture (Boronkay & Doutsos, 1994; Faure et al., 1991; Kokkalas & Aydin, 2013; Kumerics et al., 2005; Laurent et al., 2015; Ring, 2007). According to the high-resolution field mapping performed by Laurent et al. (2015; Figure 8c), the still undamaged magmatic textures from both magmatic bodies have been solely identified in the southwestern corner of the island. There, aside from the southernmost coastal area where no preferred mineral orientations have been determined, outcropping rocks distinctively show mesoscopic fabrics featured by oblate symmetries, steeply dipping foliations and constant north trending mineral lineations. These synmagmatic fabrics are gradually replaced to the north by a postsolidus noncoaxial shearing, asymmetrically distributed throughout the entire ductilely affected domain (Figure 8c). Overall, the finite strain continuously intensifies when approaching the Fanari-Gialiskari detachment plane (Figure 5b). Along a 300- to 500-m-thick ductile strain gradient, Laurent et al. (2015) have indeed divided northward and upward the successive recording of incipiently sheared magmatic rocks, then protomylonites, and finally mylonites turned into massive ultramylonites through a thin horizon of a few meters at the vicinity of the Gialiskari-Fanari detachment (Figure 8c). Within the whole sheared domain, foliation traces dip at gentler angles ($<30°$) than those measured in the southern magmatic fabrics and their interpolated trajectories have underscored at map scale a convolute profile carrying NE directed long axes and typical wavelengths of up to several kilometers. In spite of the change of foliation orientation, stretching lineations keep a stable north directed trend or slightly deflected toward a northeaster direction into the (ultra)mylonitic rocks. Either way, all assorted kinematic indicators have pointed out an unambiguous top-to-the-north or top-to-the-NE shear sense.

In addition to the above described knife-sharp fault surface of the Gialiskari-Fanari detachment, evidence of a deformational regime shift toward a more brittle-cataclastic behavior are displayed (1) at various points of the nested magmatic complex where conjugate sets of west striking, high- to low-angle normal faults have formed in response to an ongoing north to NE oriented extension, and (2) immediately underneath the Gialiskari-Fanari detachment with the observation of hydrothermally altered cataclasites (Laurent et al., 2015). With an apparent thickness reaching approximately 10 m, these foliated and faulted cataclasites typically contain rock fragments derived from (ultra)mylonites. A comparable evolution of a viscous-to-cataclastic flow has been also emphasized within a thinner section of a few hundred meters toward the western coastal sector (near Apokofto Bay, location in Figure 8c), sign of a spatial closeness with the sinuous Gialiskari-Fanari detachment most certainly located offshore west of the island.

4.4. The Naxos Monzogranite

Like on Tinos and Ikaria islands, Naxos brings together two types of granitoids with (1) a cluster of small-scale, S-type leucogranites intrusive into the northern half of the H*T* dome in close association with the migmatitic core and (2) a larger I-type intrusion typified by a compositional spectrum ranging from a hornblende-biotite monzogranite in the inner part, to a subordinate peripheral granodiorite invaded by a composite cortege of isolated and swarms of enclaves (for simplification purposes, we consider the I-type body as a monzogranite in Figure 3e and in the following text; Altherr et al., 1982; Altherr & Siebel, 2002; Jansen, 1973; Keay, 1998; Pe-Piper, 2000; Pe-Piper et al., 1997; Wijbrans & McDougall, 1988). Magmatic inclusions have been recurrently reported close to the eastern rim where a north striking, folded intrusive contact extends over ~10 km long (Figure 8d). The northern roof of the monzogranite is cut by the corrugated Moutsouna detachment (Brichau et al., 2006; Gautier et al., 1993; John & Howard, 1995; Lister et al., 1984).

As a whole, the underlying monzogranite offers an extensive array of structures and fabrics heterogeneously acquired under magmatic, ductile or brittle conditions depending upon the structural position of intrusive rocks with respect to the Moutsouna detachment (Figure 8d). The primary magmatic textures are found in the southern internal portion of the monzogranite, far from the Moutsouna detachment surface. There, a vast majority of outcropping rocks reveal a quite clear mesoscopic fabric marked by north to NW trending mineral lineations and relatively low dipping foliations ($<30°$) that tend to become steeper (dip angles of about 40–60°)

farther southeast. Toward the marginal zones, these magmatic fabrics are progressively replaced by a top-to-the-north ductile shearing (Figure 8d). At the map scale, the overall attitude of tectonic foliations supports a dome-shaped structure through which the intensity of deformation gradually increases toward the carapace. However, the most intensely deformed zone predominantly concentrates toward the north, in the vicinity of the Moutsouna detachment. Here an upward and northward gradient of shearing is observed along a 300- to 500-m-thick section, from a weakly deformed monzogranite up to a mylonitized intrusive rock associated with frequent 1- to 5-cm-thick anastomosing ultramylonite bands. An equivalent shear strain gradient can be also locally distinguished in the southeastern part of the monzogranite where the highest altitude zone culminates into pervasively foliated mylonites.

Up to approximately several tens of meters underneath the Moutsouna detachment plane, the monzogranite was ultimately reworked by an increasingly intense brittle/cataclastic deformation northward and upward, moving up from fault rocks and protocataclasites in which fragments from the underlying mylonitized carapace have been preserved, to cohesively foliated ultracataclasites directly beneath the locally observed detachment gouge. When it can be distinguished, the detachment fault surface also bears displacement clues in the brittle field under a coherent NE oriented extension (e.g., slickenline lineations, corrugations, and tension gashes).

4.5. The Serifos Granodiorite

The Late Miocene I-type intrusion over Serifos Island has been petrologically ascribed to a biotite-hornblende granodiorite (Altherr et al., 1982; Altherr & Siebel, 2002; Stouraiti et al., 2010), a relatively small scale body defined by a subtle textural zoning wherein an inner fine-grained facies has been differentiated from a marginal coarse-grained facies (Figure 3f; Rabillard et al., 2015; Salemink, 1985). Among the Cycladic I-type granitoids, the Serifos granodiorite encloses one of the richest collections in magmatic inclusions with disseminated remnants of monogenic/polygenic swarms of enclaves, dike-like monogenic swarms, or compositionally heterogeneous synplutonic dikes (Iglseder et al., 2009; Rabillard et al., 2015). Most of these composite occurrences crop out in the topographically deeper zones, in particular, all along the southern and eastern rims where the granodioritic body was in addition transected by a series of major extensional structures, namely, the Vaghia and Aghios Sostis detachments (Figures 3f and 8e; Grasemann & Petrakakis, 2007; Rabillard et al., 2015; Tschegg & Grasemann, 2009).

According to the structural observations from the above referenced fieldworks, both detachments acted over time in similar fashion involving the development of an extremely localized shearing and a subsequent evolution toward a more brittle attitude by way of low-angle normal faulting. As displayed in the distribution map of strain intensity (Figure 8e), the Vaghia and Aghios Sostis detachments brittlely juxtapose a metasomatized and weakly deformed granodiorite atop a mylonitic band not thicker than a few meters or even directly against penetratively foliated ultramylonites underneath the Aghios Sostis detachment fault. These intensely sheared rocks structurally belong to the uppermost level of a sharp gradient of shearing, that is, a narrow domain reaching a few tens to a hundred of meters in thickness through which the intensity of the bulk foliation smoothly decreases toward the inner parts of the granodiorite. With the decreasing magnitude of ductile deformation, it has also been documented an obvious evolution of the fabric-related symmetry ranging from strongly oblate mylonites to a rather more prolate shape into incipiently sheared intrusive rocks. Despite a fluctuant pattern of foliation trajectories throughout the ductilely deformed part of the intrusion, both the measured stretching and mineral lineations systematically trend toward the southwest and kinematic indicators homogeneously show a top-to-the-SW shearing.

As the extensional shearing turns out to be strongly localized, a significant portion of the granodiorite has therefore preserved magmatic textures without any substantial solid-state overprint (Rabillard et al., 2015). The magmatic domain primarily covers the central part of the intrusive body, as well as its northern edge along which a staircase-shaped intrusive contact cuts across the preexisting regional fabric. In the field, mesoscopic fabrics from both the fine-grained and coarse-grained facies appear indistinguishable or dimly expressed. Combined with an AMS survey (Rabillard et al., 2015), the magnetic and mesoscopic foliations delineate a coherent concentric pattern with a slight shape eccentricity depicted by a SW directed long axis (Figure 8e). Conversely, lineations define a more complex pattern, including a preponderant set of south to southwest trends and a second one characterized by perpendicular, east trending lineations.

5. Discussion

5.1. Finite Strain Patterns in the Cycladic Granitoids: Evidences for Magma-Assisted Strain Localization Along Detachments

One barrier in studying the state of finite strain within deformed intrusive bodies is that clues for the initial magmatic state are often partially or completely obliterated by a superimposed solid-state deformation. However, the accumulated high-shear strain can be sufficiently localized within a narrow domain so that primary magmatic textures and incipient stages of deformation can be preserved underneath. In particular, magmatic fabrics received increasing attention since they represent a foreground importance for determining fabric-forming processes that operated during the early to subsolidus states of magma crystallization. According to classical interpretations, magmatic fabrics may originate either from intrinsic (e.g., pressure-driven magmatic flows or emplacement-related conditions) or extrinsic processes (e.g., regional stress regime; Paterson et al., 1998, 1989; Vernon, 2000). The finite structure of a pluton can be interpreted either as a record of deformation (due to emplacement dynamics or to regional deformation) or as a magmatic record of magma differentiation during successive injection pulses (de Saint Blanquat et al., 2011). In other words, the synkinematic character of granitoids strongly depends on the degree of coupling between magmatic and host rocks fabrics.

The qualitative field-based mapping of the state of finite strain performed over the five Cycladic magmatic complexes (Tinos, Mykonos-Delos-Rhenia, Ikaria, Naxos, and Serifos) yields insight for both the distribution and the evolution of deformation for each case study. Independently of radiometric time constraints, the systematic structural mapping through the synextensional intrusions more precisely testifies to their synkinematic nature. The compilation of our structural data with already published ones clearly shows a continuum of deformation from magmatic to solid-state ductile conditions and finally toward a more brittle/cataclastic behavior (Figure 8). Furthermore, kinematics observed throughout lateral ductile shear gradients are entirely compatible with those recorded within corresponding metamorphic domes and especially on approaching the detachment zones. Although time constants between short-time intrusive events and long-lasting detachment activities are quite different, comagmatic deformation (or orientation of the flow) and subsolidus deformation recorded during cooling show a progressive localization toward the detachment planes that cap intrusion roofs. The alignment of magmatic minerals and their stretching (K-feldspars) at the late magmatic stage is always parallel to the regional stretching direction associated with the normal displacement along the detachments. The direction of the magmatic flow (mainly inferred from the direction of the mineral lineation; e.g., Paterson et al., 1989; and alignment of K-feldspars) thus seems in the great majority of cases entirely oriented by the regional strain and stress field (i.e., Mykonos, Ikaria, and Naxos). A more complex pattern is, however, inferred from Tinos and Serifos intrusions, especially in magmatic domains where AMS fabrics do not always mimic mineral fabrics. The complex trend has been exclusively recorded by AMS signal and was tentatively interpreted as emplacement-related magma infilling along NW-SE oriented tensional zones whose direction of opening could be consistent with the NE-SW directed regional extension (de Saint Blanquat et al., 2011; Rabillard et al., 2015). For instance, the importance of the coalescence of dikes striking perpendicular to the regional stretching direction to form the intrusive body is well illustrated by the southernmost part of the Tinos intrusion. The exact mechanism that links comagmatic flow and subsolidus deformation remains to be ascertained, but the example of Serifos shows that the magma is deformed while still viscous in the direction of regional shearing enlightening a continuum of shearing from the late magmatic stage to subsolidus deformation. This is indeed suggested by protodikes of mafic rocks invading the root zone of the pluton that are dismembered to give mafic enclaves downstream (Rabillard et al., 2015).

Overall, structural investigations both inside and outside synextensional granitoids provide new insights into geological processes through which the Cycladic intrusions have spatially interacted through time with strain localization events. It seems that the bulk architectures and cooling (i.e., the apparent rejuvenation of cooling ages toward detachment planes) of the Cycladic granitoids were tectonically controlled by a contemporaneous noncoaxial shearing that localized over time into detachments through their upper intrusive contacts. This is illustrated by the overall asymmetrical geometries of all these plutons, the most typical of this behavior being Serifos and Ikaria. This picture thus significantly differs from some previous studies in which the relations between tectonism and magmatism were also investigated at regional scale (Boronkay & Doutsos, 1994; Kokkalas & Aydin, 2013; Koukouvelas & Kokkalas, 2003). Even if the aforementioned authors recognized that the Cycladic granitoids are spatially associated with low-angle normal faults, they rather concluded that

late-stage emplacements and ensuing deformations were primarily controlled by systems of transtensional strike-slip faults. Although strike-slip faults can be recorded over some islands (Naxos, Ikaria, and Mykonos), such structures obviously crosscut both across detachments and granitoids and thereby started to localize later than the activity of the detachments and I-type magmatism (Beaudoin et al., 2015; Menant et al., 2013; Siebenaller, 2008).

5.2. Relations Between Magmatism, Exhumation Processes and Detachment Faulting: Toward a Coherent Regional Scheme

In the Cycladic archipelago, one of the most striking features in reviewing the granitoid-cored MCCs is their ubiquitous association with multiple and closely spaced detachments. Such architectural configuration thus raises the question of how these synkinematic granitoids could have been over time geometrically paired with those detachment systems and it brings us back to the link between syntectonic magmatism, exhumation processes of deep crustal rocks, and detachment faulting.

A part of this question has, however, been already answered as the detachments have a much longer history than the plutons (Figure 2). Through (U-Th)/Pb radiometric ages reported from the Cycladic granitoids, it seems now well constrained that the magmatic activity took place only in the late exhumation stages of metamorphic domes (Bolhar et al., 2010; Brichau et al., 2008, 2007; Iglseder et al., 2009; Keay, 1998; Keay et al., 2001). The surge of intrusive magmatism, including I- and S-type granitoids, was indeed limited into a relatively short time window (15–9 Ma), while the deeply buried metamorphic rocks from the Hellenic accretionary wedge were already experiencing an overall exhumation-related retrograde metamorphism under greenschist-facies conditions (Figure 2). It can thus be concluded that none of those intrusions appears to be a viable candidate for the genesis of MCCs but would rather be a consequence of a warmer geodynamic environment during lithospheric thinning and slab retreat (Jolivet et al., 2015). In the wake of a faster southward rollback of the subduction front (since 35–30 Ma) and probably a subsequent progressive tearing of the subducting Hellenic slab (between 20 and 16 Ma), the arrival of a hot asthenospheric flow would have therefore progressively replaced the overlying lithosphere, thereby providing a sufficient heat input for a partial melting of the extending lower crust and the metasomatized mantle wedge (Jolivet et al., 2015; Menant, Jolivet, & Vrielynck, 2016). With ongoing extension, S- and I-type magmas generated in the mantle and the deep crust were partly dragged upward through the crust and then accumulated into already formed MCCs in which detachment faulting was at a mature stage. As a result, some authors tentatively concluded that crustal-scale detachments could behave successively as ready pathways for magma migration through the crust and active mechanical barriers below which composite magmatic bodies were efficiently trapped, stored, and quite simply deformed during their subsequent cooling (Bolhar et al., 2010; Brichau et al., 2008, 2007, 2010). The field relations described in the present paper show instead that, while they indeed act as mechanical barriers and deeply influence the geometry and deformation of ascending and cooling plutons, the detachments are not pathways for magmas.

As further shown above, the present-day anatomies of the granitoid-cored metamorphic domes, however, imply somewhat more complex exhumation histories with the development of multiple detachments. Even if the exact onset of each MCC-bounding detachment remains uncertain through radiometric dating, some key elements reported in this review tend to demonstrate successively active detachments as a result of local and transient interactions with granitoid intrusions, rather than their concomitant existence, as shown in Figure 9. All structural, kinematic, and geometrical constraints indeed converge upon a coherent model in which the exhumation of the granitoid-cored domes was systematically achieved below a single detachment that was inactivated at the time of intrusion and replaced by a new strain localization zone at the upper intrusive contact of the granitoids.

Such a tectonic scheme has been already proposed for the final exhumation stages of both the Tinos and Mykonos domes along which the sequential generation of three detachments of the NCDS was punctuated by successive and discrete pulses of magma batches (Jolivet et al., 2010). There, the top-to-the-NE deformation was first progressively localized along the Tinos detachment since ~30 Ma (detachment 1 in Figure 9). It was essentially active in the ductile field and evolved as a brittle detachment before it was intruded and locally inhibited by the Tinos magmatic complex at circa 15–14 Ma. The monzogranite intruded the dome at relatively upper crustal depths (related-crystallization pressure estimations: 300–400 MPa; Bröcker & Franz, 1994) and concurrently produced a thermal weakening of surrounding rocks as well as a strain

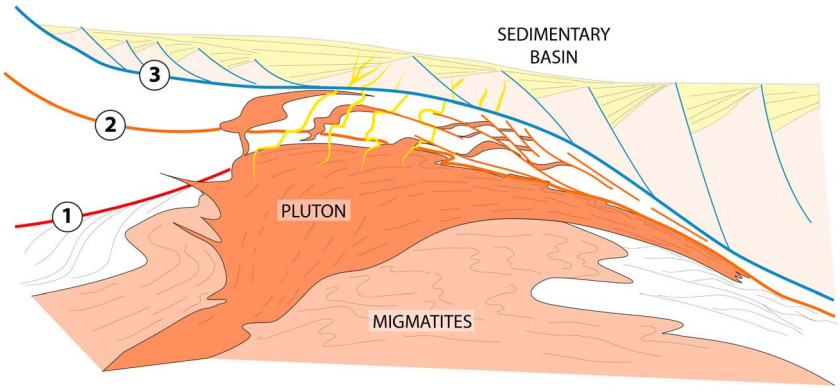

Figure 9. Cross section showing the sequentially developed detachment branches as resulting from the local interaction with a granitoid intrusion. This sketch can easily be used for each late exhumation history of metamorphic domes described in this study. The pluton intrudes an already active metamorphic core complex topped with a detachment (1) associated with or without a migmatite dome in its core. The early formed detachment can be the equivalent to the Tinos, Agios-Kirykos, Naxos, or Meghàlo Livadhi detachments. The intrusion inactivates the early detachment that is replaced by a new detachment (2) localizing along the upper contact of the pluton, similar to the Livada, Gialiskari-Fanari, Moutsouna, or Kàvos Kiklopas detachments. A shear zone develops within the pluton with a continuum of deformation from the comagmatic flow to subsolidus colder deformation and mylonitization below the new detachment. Finally, a third detachment may form above, strictly in brittle-cataclastic behavior, and its complete the exhumation of the metamorphic core complex, like the Mykonos detachment.

reactivation in ductile condition. Extensional shearing migrated both along the intrusion roof and its upper margin, still under a NE directed extensional regime. The shear strain was then gradually localized through the Livada detachment along the intrusive contact of the 14- to 11-Ma-old Mykonos sheeted complex and also likely at the apex of the Tinos monzogranite (detachment 2 in Figure 9). Once the granitoids were cold, extensional deformation evolved toward a more brittle-cataclastic behavior and was transferred along the Mykonos detachment at the interface between the MCC and overlying sedimentary basins (detachment 3 in Figure 9).

This evolution can be seen almost with the same sequence on Ikaria where the magmatic event actively contributed in shaping the present-day architecture of the migmatite-cored MCC (Beaudoin et al., 2015; Laurent et al., 2015). The exhumation of the H*T* metamorphic dome was governed by an overall north directed extension and completed by two anastomosing high-strain zones, that is, the deeper Agios-Kirykos shear zone and the late and more surficial Gialiskari-Fanari low-angle normal fault. The top-to-the-north strain localization along the Agios-Kirykos shear zone would have started before or simultaneously with the H*T* episode of partial melting (~16 Ma) and lasted until it was pierced and sealed by early intrusions of the composite magmatic system (15–13 Ma) at midcrustal level (related-crystallization pressure estimations: 300–500 MPa; Laurent et al., 2015). The extensional deformation then migrated at the top of the Raches monzogranite and lastly localized with time under ductile-to-brittle/cataclastic conditions along the newly formed Gialiskari-Fanari detachment fault. An analogous tectonic history for the NPDS can also be drawn farther south on Naxos, where the migmatite-cored metamorphic dome was successively exhumed below the ductile-to-brittle Naxos detachment and then below the more localized ductile-to-brittle Moutsouna detachment. Associated with a stable top-to-the-north kinematic, the onset of extensional shearing and subsequent strain localization along the deeper Naxos detachment branch would have preceded and coincided with the peak of H*T* (~21–17 Ma). It predominantly operated in ductile condition and ended as an extensional brittle detachment prior to the 13- to 11-Ma old I-type intrusion. Magmatic products were emplaced into the hanging wall of the Naxos detachment at upper crustal depths (200–300 MPa; Cao et al., 2017; Gautier et al., 1993; Jansen & Schuilling, 1976) and had temporarily disturbed both the thermal structure and the deformational regime prevailing within the surrounding system. The resulting ductile shearing was ultimately transferred upsection where the Moutsouna detachment localized along the intrusive margin. In the same way on Serifos, extension-related exhumation of the metamorphic dome was initially accommodated by a single detachment branch of the WCDS that was afterward blocked and substituted by new detachment zones as the result of magmatic activity. From the Middle Miocene onward, the top-to-the-SW shearing was

indeed first concentrated along the Meghàlo Livadhi detachment under ductile-then-brittle conditions before being intruded and sealed by the ~11- to 9-Ma-old granodioritic body at shallow crustal level (approximately 300 MPa; St. Seymour et al., 2009). In a short time span, the granodioritic intrusion radically altered the local temperature, reheating host rocks and inducing some ductile deformation under an unchanging stress regime. Strain accommodation was thereby achieved higher up through a set of narrow high-strain zones that tended to localize both at the intrusion roof (i.e., Agios Sostis and Vaghia detachments) and into adjacent host rocks (i.e., Kàvos Kiklopas detachment). Given structural and kinematic similitudes between the newly formed detachment zones, one can assume that those three branches were contemporaneous and most likely genetically linked as a unique detachment.

Concluding, these similar sequences of events are thus not a local characteristic of the NCDS but it seems to reveal a general behavior of detachments systems interfering with intrusions. Instead of a passive attitude with regard to extensional tectonics, magmatic intrusions have rather dynamically impacted the late evolution stages of the Cycladic MCCs (Figure 9). The present scenarios further corroborate the fact that the strength evolution of the crust in MCC-type systems can become nonlinear and cyclical with the arrival of episodic and repeated pulses of magma. Partially crystallized plutonic bodies, behaving as transient thermomechanical instabilities, may indeed introduce short-lived rheological contrasts and induce weakening and then hardening of the upper continental crust.

5.3. Mechanical Implications

The same succession of events is thus observed during the emplacement of the Aegean plutons, which ascent is associated with an upward migration of associated detachments in the crust. This observation raises several questions:

One first important question is the mechanism by which the pluton intrudes through the detachment, how does such a weak material pearces the mechanical discontinuity of the detachment and intrudes the upper unit, forming shallow-dipping sheets of magma. The examples of Tinos and Mykonos might provide part of the answer. In both cases the interface between the main granitic body and the host rock is associated with dikes and sills that intrude the foliation or cut through it. A possibility is then that the brittle formation of shallow and steeptly dipping veins opens the way for the main magma (Figure 9).

A second important question is why the injection of magma makes the detachement migrate upward within the upper plate when one would think that the weak magma localizes deformation. If one leaves aside the possibility that shearing deformation was distributed through the whole magmatic body and is thus impossible to observe, two solutions may be proposed. The first idea is that shearing localizes where the strongest rheological contrast is observed, that is, at the contact between the weak magma and the resistant upper unit. The second possibility is that the pluton heats up the upper unit and thus lowers its strenght, thus rising the ductile-brittle transition migrating upward (Jolivet & Patriat, 1999).

A third question is why does the detachment migrate upward after cooling of the pluton and not downward as proposed by de Saint Blanquat et al. (2011) for the Tinos pluton. One can indeed argue that when the pluton intrudes the upper crust, once cold it behaves brittlely. But we see instead a further localization of deformation within the upper Mykonos Detachement during and after the deposition of the Late Miocene sediments and during the formation of the barite ore deposit at around 9–10 Ma. This is probably due to the presence of a strength contrast at the base of the basin, between the cold granite and the upper Cycladic Unit, on the one hand, and the basin on the other hand. This does not preclude that some shearing deformation was also active at depth within the brittle-ductile transition deeper down in the crust, but as exhumation stopped at that stage we have no clue about it.

In most examples we have studied, the main intrusions intrude the UCU and thus pierce the main detachment that was active before intrusion. In the case of Ikaria, as there is no strict equivalent of the UCU, one cannot be, however, so conclusive. Although the early branches of the detachments are locally inactivated when the pluton pierces through them, we do not consider that the evolution of the system of detachment was punctuated. In the case of the NCDS, for instance, the Livada Detachment corresponds to the upward migration of the Tinos Detachment along the rheological discontinuity formed at the upper limit of the pluton but, at a distance from the pluton, the Tinos Detachment was probably still active until it was relayed by the uppermost Mykonos Detachment. Rather than a punctuated evolution, we see a continuum of extension

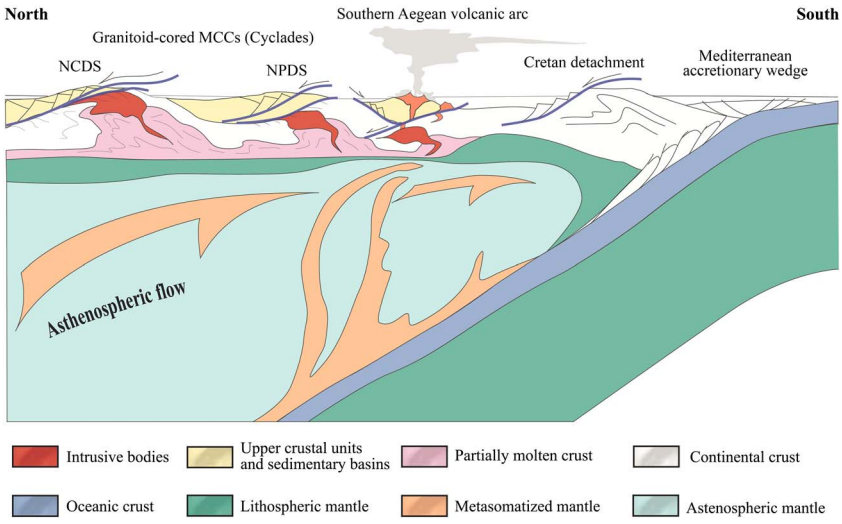

Figure 10. Speculative sketch of a retreating subduction zone with back-arc extension and emplacement of plutons below detachments during the retreat and migration of the magmatic arc. We assume that the exhumed structures observed within the exhumed MCC are a good image of the processes active below the Quaternary volcanic arc. NCDS = North Cycladic Detachment System; NPDS = Naxos-Paros Detachment System; MCCs = metamorphic core complexes.

with progressive localization toward the top. A comparison with the Plaka pluton that has interacted with the WCDS in Lavrion Peninsula (Berger et al., 2013; Scheffer et al., 2016) would be interesting as the main body of the pluton does not intrude the visible detachment, only dikes and fluids related to the intrusion intrude the upper unit. This situation might correspond a less intense extension near the northern end of the WCDS.

Finally, the different examples we have studied show that extension is not taken up by one single shear surface that was active all along but by a system of individual detachments locally interacting with plutons. The existence of the different branches on the main detachment is due to (1) the intrinsic heterogeneity of the crust where several zones of strength contrast exist (inherited nappe contacts, sediment/basement interface) and (2) to the intrusions themselves that locally modify the rheology of the host rock by raising the temperature and provide new strength contrasts along their margins during intrusion and cooling. The presence of H*T* domes associated with some of the plutons (Naxos, Mykonos, and Ikaria) have played a similar role in weakening the nappe pile during extension, at a larger scale than the simple plutons which thermal impact is limited to their immediate proximity.

5.4. Can One Expect an Analogous Tectonomagmatic Configuration Below the Southern Aegean Volcanic Arc? Some Speculations

This analysis of the interactions between the Aegean plutons and contemporaneous detachments shows strong similarities among the different studied examples. The same type of interactions is recognized over the ~5- to 6-Ma time window during which the Aegean plutons were emplaced. Magmatic activity in the Aegean region has been continuous since the Late Cretaceous when the magmatic arc was located much further north in the Balkans. It then migrated progressively southward with acceleration some 35 Ma following slab retreat. The emplacement of the Aegean granites is partly related to this southward migration and to a slab tearing event that is postulated between 15 and 9 Ma (Jolivet et al., 2015), which is during the same period. The magmatic arc then continued to migrate southward to reach its present position. The question can then be posed for the continuation of the same emplacement dynamics in the recent period, below the active arc, as during the Miocene.

Figure 10 proposes a speculative sketch of a migrating magmatic arc above a retreating subduction. This model is inspired from the interrelations between the Aegean intrusions and the multiple sets of associated detachments described above. It also benefited a lot from numerical modeling of Menant, Sternai, et al. (2016) that shows the dynamics of mantle flowing between the retreating slab and the upper plate. Leaving aside the 3-D complexity of this flow in Menant, Sternai, et al. (2016), we simply retain the

geometry of partially molten mantle plume above the subducting slab. The flow induced by slab retreat is southward, and the coupling between the flow and the deforming crust above leads to an asymmetrical deformation with north dipping detachments exhuming crustal boudins and MCCs (Jolivet, Famin, et al., 2004; Jolivet et al., 2013, 2009). A steady state slab migration leads to a migration of the volcanic arc at a constant velocity. The observation that the Serifos pluton central facies is finer grained may suggest that it was emplaced, while the magmatic chamber was opened toward the surface, thus calling for the presence of a volcano above (Rabillard et al., 2015). Volcanic rocks contemporaneous with the Serifos pluton can be found only in the eastern part of the Aegean Sea (Pe-Piper & Piper, 2006), and they cannot be anything directly associated with that pluton. One may, however, argue that the volcanic equivalent of the Serifos pluton should be looked for offshore south of the island, where they should have been displaced by the activity of the detachments. One may then assume the same geometry for the Naxos pluton and all the Aegean plutons. This assumed continuum is reasonable (but not proven) in the light of the comparison between the direction of Miocene shearing direction and active Global Positioning System displacements in the Aegean domain (Jolivet, 2001). This is of course highly conjectural as these volcanoes would be preserved in the upper unit, above the detachment, and have thus been displaced by the later motion along the detachment. One may finally postulate that the same geometry and connections between the pluton and the volcano is at work below the present volcanic arc. Some recent seismic tomography model (Dimitriadis et al., 2010, see their Figure 15) suggests the presence of a H*T* anomaly below Santorini, dipping toward the NE down to 5–8 km. This anomaly could sign the presence of a connected magmatic system down to that depth and its northeastward dip could be an image of a NE dipping detachment. If this highly speculative model holds, it means that, during southward slab retreat, the deep parts of similar pluton-volcano systems were progressively exhumed in the back-arc region. The plutonic complexes of Naxos, Serifos, Ikaria, Mykonos, and Tinos would then provide images of the plutonic system presently active below Santorini.

6. Conclusion

The analysis in the field of five Aegean plutons (Tinos, Mykonos, Ikaria, Naxos, and Serifos) reveals closely similar evolutions during their emplacement. The interactions between these synkinematic granitoids and the detachments responsible for the exhumation of the MCCs and more generally the H*P* metamorphic rocks in which they intrude show the same sequence of events. These magmatic bodies intrude a MCC that is already forming below a large-scale detachment, the NCDS, the WCDS, or the NPDS. They intrude these MCCs in a quite late stage of their evolution and are thus not the cause for the localization of extension. Granitoids intrude a first generation of detachments that is then inactivated and replaced by a new strain localization zone along the upper contact of the intrusion with its host rock. A ductile shear zone develops within the granitoid with a marked strain gradient toward the new detachment that finally evolves toward a brittle behavior. This detachment may then be in turn replaced by an additional brittle detachment forming higher up in the crust and completing the exhumation of the MCC.

Within the intrusion, a continuum of shearing deformation is observed from the comagmatic flow to the subsolidus deformation and the formation of a thick mylonitic zone evolving into cataclasites. The shearing direction at the magmatic stage and during the subsequent colder deformation and mylonitization are parallel showing that the magmatic flow is oriented by the regional deformation pattern in this case. The exact mechanism that controls the flow of magma in such environments remains to be understood.

Finally, we speculate on a possible connection between the present-day Hellenic volcanic arc and potential granitic magmas at depth, assuming that the kinematics of detachments seen for the Miocene record in the Cyclades is still prevailing at depth below Santorini. We further propose that the MCCs exhumed in the Cyclades during slab retreat are a potential equivalent of the active plutons below the present-day volcanic arc.

Acknowledgments
This paper is a contribution of the ERC RHEOLITH Project (ERC advanced Grant 290864) and Labex VOLTAIRE (Convention ANR-10-LABEX-100-01). The authors are indebted to IGME and especially to Nikolas Carras and Adonis Photiades for their help. Michel de Saint-Blanquat and Konstantinos Soukis should also be sincerely thanked for their insightful and constructive reviews.

References

Altherr, R., Kreuzer, H., Lenz, H., Wendt, I., Harre, W., & Dürr, S. (1994). Further evidence for a Late Cretaceous low-pressure/high-temperature terrane in the Cyclades, Greece. *Chemie der Erde*, *54*, 319–328.

Altherr, R., Kreuzer, H., Wendt, I., Lenz, H., Wagner, G. A., Keller, J., et al. (1982). A Late Oligocene/Early Miocene high temperature belt in the anti-cycladic crystalline complex (SE Pelagonian, Greece). *Geologische Jachbuch*, *23*, 97–164.

Altherr, R., & Siebel, W. (2002). I-type plutonism in a continental back-arc setting: Miocene granitoids and monzonites from the central Aegean Sea, Greece. *Contributions to Mineralogy and Petrology*, *143*(4), 397–415. https://doi.org/10.1007/s00410-002-0352-y

Andriessen, P. A. M. (1991). K-Ar and Rb-Sr age determinations on micas of impure marbles of Naxos, Greece: The influence of metamorphic fluids and lithology on the blocking temperature. *Schweizerische Petrologie und Mineralogie Mitteilungen*, *71*(8), 89–99.

Andriessen, P. A. M., Banga, G., & Hebeda, E. H. (1987). Isotopic age study of pre-Alpine rocks in the basal units on Naxos, Sikinos and Ios, Greek Cyclades. *Geologie en Mijnbouw*, *66*, 3–14.

Andriessen, P. A. M., Boelrijk, N. A. I. M., Hebeda, E. H., Priem, H. N. A., Verdurmen, E. A. T., & Vershure, R. H. (1979). Dating the events of metamorphism and granitic magmatism in the Alpine orogen of Naxos (Cyclades, Grèce). *Contributions to Mineralogy and Petrology*, *69*, 215–225. https://doi.org/10.1007/BF00372323

Angelier, J., Glaçon, G., & Muller, C. (1978). Sur la présence et la position tectonique du Miocène inférieur marin dans l'archipel de Naxos (Cyclades, Grèce). *Comptes Rendus de l'Académie des Sciences Paris*, *286*, 21–24.

Armstrong, R. L. (1982). Cordilleran metamorphic core complexes, from Arizona to southern Canada. *Annual Review of Earth and Planetary Sciences*, *10*, 129–154. https://doi.org/10.1146/annurev.ea.1110.0501805012.001021

Armstrong, R. L., & Ward, P. (1991). Evolving geographic patterns of Cenozoic magmatism in the North American Cordillera: The temporal and spatial association of magmatism and metamorphic core complexes. *Journal of Geophysical Research*, *96*, 13,201–13,224. https://doi.org/10.11029/13291JB00412

Aubouin, J. (1959). Contribution à l'étude de la Grèce septentrionale; les confins de l'Epire et de la Thessalie. *Annales Géologiques des Pays Helléniques*, *10*, 1–483.

Augier, R., Choulet, F., Faure, M., & Turrillot, P. (2015). A turning-point in the evolution of the Variscan orogen: The ca. 325 Ma regional partial-melting event of the coastal South Armorican domain (South Brittany and Vendée, France). *Bulletin de la Société Géologique de France*, *186*(2–3), 63–91. https://doi.org/10.2113/gssgfbull.2186.2112-2113.2163

Augier, R., Jolivet, L., Gadenne, L., Lahfid, A., & Driussi, O. (2015). Exhumation kinematics of the Cycladic Blueschists Unit and back-arc extension, insights from the Southern Cyclades (Sikinos and Folegandros Islands, Greece). *Tectonics*, *34*, 152–185. https://doi.org/10.1002/2014TC003664

Avigad, A., Garfunkel, Z., Jolivet, L., & Azañón, J. M. (1997). Back-arc extension and denudation of Mediterranean eclogites. *Tectonics*, *16*, 924–941. https://doi.org/10.1029/1097TC02003

Avigad, D. (1998). High-pressure metamorphism and cooling on SE Naxos (Cyclades, Greece). *European Journal of Mineralogy*, *10*(6), 1309–1320. https://doi.org/10.1127/ejm/10/6/1309

Avigad, D., Baer, G., & Heimann, A. (1998). Block rotations and continental extension in the Central Aegean Sea: Paleomagnetic and structural evidence from Tinos and Mykonos. *Earth and Planetary Science Letters*, *157*, 23–40. https://doi.org/10.1016/S0012-1821X(1098)00024-00027

Avigad, D., & Garfunkel, Z. (1989). Low-angle faults above and below a blueschist belt: Tinos Island, Cyclades, Greece. *Terra Nova*, *1*, 182–187. https://doi.org/10.1111/j.1365–3121.1989.tb00350.x

Avigad, D., Ziv, A., & Garfunkel, Z. (2001). Ductile and brittle shortening, extension-parallel folds and maintenance of crustal thickness in the Central Aegean. *Tectonics*, *20*, 277–287. https://doi.org/10.1029/2000TC001190

Baldwin, S. L., & Lister, G. S. (1998). Thermochronology of the South Cyclades Shear Zone, Ios, Greece: Effects of ductile shear in the argon partial retention zone. *Journal of Geophysical Research*, *103*, 7315–7336. https://doi.org/10.1029/7397JB03106

Baldwin, S. L., Lister, G. S., Hill, E. J., Foster, D. A., & McDougall, I. (1993). Thermochronologic constraints on the tectonic evolution of active metamorphic core complexes, D'entrecasteaux Islands, Papua New Guinea. *Tectonics*, *12*, 611–628. https://doi.org/10.1029/1093TC00235

Bargnesi, E. A., Stockli, D. F., Mancktelow, N., & Soukis, K. (2013). Miocene core complex development and coeval supradetachment basin evolution of Paros, Greece, insights from (U–Th)/He thermochronometry. *Tectonophysics*, *595-596*, 165–182. https://doi.org/10.1016/j.tecto.2012.1007.1015

Beaudoin, A., Augier, R., Laurent, V., Jolivet, L., Lahfid, A., Bosse, V., et al. (2015). The Ikaria high-temperature metamorphic core complex (Cyclades, Greece): Geometry, kinematics and thermal structure. *Journal of Geodynamics*, *92*, 18–41. https://doi.org/10.1016/j.jog.2015.1009.1004

Berger, A., Schneider, D. A., Grasemann, B., & Stockli, D. (2013). Footwall mineralization during Late Miocene extension along the West Cycladic Detachment System, Lavrion, Greece. *Terra Nova*, *25*(3), 181–191. https://doi.org/10.1111/ter.12016

Bessière, E., Rabillard, A., Précigout, J., Arbaret, L., Jolivet, L., Augier, R., et al. (2017). Strain localization within a syn-tectonic intrusion in a back-arc extensional context: The Naxos monzogranite (Greece). *Tectonics*, *37*, 558–587. https://doi.org/10.1002/2017TC004801

Beyssac, O., Goffé, B., Chopin, C., & Rouzaud, J. N. (2002). Raman spectra of carbonaceous material from metasediments: A new geothermometer. *Journal of Metamorphic Geology*, *20*, 859–871. https://doi.org/10.1046/j.1525–1314.2002.00408.x

Blake, M. C., Bonneau, M., Geyssant, J., Kienast, J. R., Lepvrier, C., Maluski, H., & Papanikolaou, D. (1981). A geological reconnaissance of the Cyclacic blueschist belt, Greece. *Bulletin Geological Society of America*, *92*, 247–254. https://doi.org/10.1130/0016–7606(1981)1192<1247:AGROTC>1132.1130.CO;1132

Bohnhoff, M., Rische, M., Meier, T., Becker, D., Stavrakakis, G., & Harjes, H. P. (2006). Microseismic activity in the Hellenic volcanic arc, Greece, with emphasis on the seismotectonic setting of the Santorini–Amorgos zone. *Tectonophysics*, *423*(1–4), 17–33. https://doi.org/10.1016/j.tecto.2006.1003.1024

Bohnhoff, M., Rische, M., Meier, T., Endrun, B., Becker, D., Harjes, H. P., & Stavrakakis, G. (2004). CYC-NET: A temporary seismic network on the Cyclades (Aegean Sea, Greece). *Seismological Research Letters*, *75*(3), 352–359. https://doi.org/10.1785/gssrl.1775.1783.1352

Bolhar, R., Ring, U., & Allen, C. M. (2010). An integrated zircon geochronological and geochemical investigation into the Miocene plutonic evolution of the Cyclades, Aegean Sea, Greece: Part 1: Geochronology. *Contributions to Mineralogy and Petrology*, *160*, 719–742. https://doi.org/10.1007/s00410–00010–00504-00414

Bolhar, R., Ring, U., Kemp, A. I. S., Whitehouse, M. J., Weaver, S. D., Woodhead, J. D., et al. (2012). An integrated zircon geochronological and geochemical investigation into the Miocene plutonic evolution of the Cyclades, Aegean Sea, Greece: Part 2: Geochemistry. *Contributions to Mineralogy and Petrology*, *164*(6), 915–933. https://doi.org/10.1007/s00410-012-0759-z

Bonini, M., Sokoutis, D., Mulugeta, G., Boccaletti, M., Corti, G., Innocenti, F., et al. (2001). Dynamics of magma emplacement in centrifuge models of continental extension with implications for flank volcanism. *Tectonics*, *20*, 1053–1065. https://doi.org/10.1029/2001TC900017

Bonneau, M. (1984). Correlation of the Hellenic nappes in the south-east Aegean and their tectonic reconstruction. In J. E. Dixon & A. H. F. Robertson (Eds.), *The geological evolution of the Eastern Mediterranean* (pp. 517–527). Oxford: Blackwell Scientific Publications. https://doi.org/10.1144/GSL.SP.11191184.1017.1101.1138

Boronkay, K., & Doutsos, T. (1994). Transpression and transtension in different structural levels in the Central Aegean region. *Journal of Structural Geology*, *16*, 1555–1573. https://doi.org/10.1016/0191–8141(1594)90033–90037

Borradaile, G. J., & Henry, B. (1997). Tectonic applications of magnetic susceptibility and its anisotropy. *Earth-Science Reviews*, *42*(1–2), 49–93. https://doi.org/10.1016/S0012-8252(1096)00044-X

Borradaile, G. J., & Jackson, M. (2010). Structural geology, petrofabrics and magnetic fabrics (AMS, AARM, AIRM). *Journal of Structural Geology*, *32*(10), 1519–1551. https://doi.org/10.1016/j.jsg.2009.1509.1006

Bouchez, J. L., Delas, C., Gleizes, G., Nédélec, A., & Cuney, M. (1992). Submagmatic microfractures in granites. *Geology*, *20*(1), 35–38. https://doi.org/10.1130/0091-7613(1992)1020<0035:SMIG>1132.1133.CO;1132

Bozkurt, E., & Park, R. G. (1994). Southern Menderes massif: An incipient metamorphic core complex in Western Anatolia. *Journal of the Geological Society of London*, *151*, 213–216. https://doi.org/10.1144/gsjgs.1151.1142.0213

Brichau, S., Ring, U., Carter, A., Bolhar, R., Monié, P., Stockli, D., & Brunel, M. (2008). Timing, slip rate, displacement and cooling history of the Mykonos detachment footwall, Cyclades, Greece, and implications for the opening of the Aegean Sea basin. *Journal of the Geological Society of London*, *165*, 263–277. https://doi.org/10.1144/0016–76492006-76492145

Brichau, S., Ring, U., Carter, A., Monie, P., Bolhar, R., Stockli, D., & Brunel, M. (2007). Extensional faulting on Tinos Island, Aegean Sea, Greece: How many detachments? *Tectonics*, *26*, TC4009. https://doi.org/10.1029/2006TC001969

Brichau, S., Ring, U., Ketcham, R. A., Carter, A., Stockli, D., & Brunel, M. (2006). Constraining the long-term evolution of the slip rate for a major extensional fault system in the central Aegean, Greece, using thermochronology. *Earth and Planetary Science Letters*, *241*, 293–306. https://doi.org/10.1016/j.epsl.2005.1009.1065

Brichau, S., Thomson, S., & Ring, U. (2010). Thermochronometric constraints on the tectonic evolution of the Serifos detachment, Aegean Sea, Greece. *International Journal of Earth Sciences (Geol Rundsch)*, *99*, 379–393. https://doi.org/10.1007/s00531–00008–00386-00530

Bröcker, M. (1990). Blueschist-to-greenschist transition in metabasites from Tinos island, Cyclade, Greece: compositional control or fluid infiltration. *Lithos*, *25*, 25–39. https://doi.org/10.1016/0024-4937(1090)90004-K

Bröcker, M., Bieling, D., Hacker, B., & Gans, P. (2004). High-Si phengite records the time of greenschist facies overprinting: implications for models suggesting mega-detachments in the Aegean Sea. *Journal of Metamorphic Geology*, *22*, 427–442. https://doi.org/10.1111/j.1525–1314.2004.00524.x

Bröcker, M., & Franz, L. (1994). The contact aureole on Tinos (Cyclades, Greece). Part I: field relationships, petrography and P-T conditions. *Chemie der Erde*, *54*, 262–280.

Bröcker, M., & Franz, L. (1998). Rb-Sr isotope studies on Tinos island (Cyclades, Greece): additional time constraints for metamorphism, extent of inflitration-controlled overprinting and deformational activity. *Geological Magazine*, *135*, 369–382. https://doi.org/10.1017/S0016756898008681

Bröcker, M., & Franz, L. (2000). The contact aureole on Tinos (Cyclades, Greece): Tourmaline-biotite geothermometry and Rb-Sr geochronology. *Mineralogy and Petrology*, *70*, 257–283. https://doi.org/10.1007/s007100070006

Bröcker, M., Kreuzer, H., Matthews, A., & Okrusch, M. (1993). $^{40}Ar/^{39}Ar$ and oxygen isotope studies of polymetamorphism from Tinos island, Cycladic blueschist belt, Greece. *Journal of Metamorphic Geology*, *11*, 223–240. https://doi.org/10.1111/j.1525–1314.11111993.tb00144.x

Brown, M., & Dallmeyer, R. D. (1996). Rapid Variscan exhumation and the role of magma in core complex formation: southern Brittany metamorphic belt, France. *Journal of Metamorphic Geology*, *14*(3), 361–379. https://doi.org/10.1111/j.1525–1314.1996.00361.x

Brun, J. P., & Faccenna, C. (2008). Exhumation of high-pressure rocks driven by slab rollback. *Earth and Planetary Science Letters*, *272*(1-2), 1–7. https://doi.org/10.1016/j.epsl.2008.1002.1038

Brun, J. P., & Van Den Driessche, J. (1994). Extensional gneiss domes and detachment fault systems: Structure and kinematics. *Bulletin de la Societe Geologique de France*, *165*, 519–530.

Buick, I. S. (1991a). Mylonite fabric development on Naxos, Greece. *Journal of Structural Geology*, *13*(6), 643–655. https://doi.org/10.1016/0191-8141(91)90027-G

Buick, I. S. (1991b). The late alpine evolution of an extensional shear zone, Naxos, Greece. *Journal of the Geological Society*, *148*, 93–103. https://doi.org/10.1144/gsjgs.1148.1141.0093

Buick, I. S., & Holland, T. J. B. (1989). The P-T-t path associated with crustal extension, Naxos, Cyclades, Greece. In J. S. Daly (Ed.), *Evolution of metamorphic belts* (pp. 365–369). London: Geological Society, Special Publications. https://doi.org/10.1144/GSL.SP.1989.1043.1101.1132

Burg, J. P. (2012). Rhodope: From Mesozoic convergence to Cenozoic extension. Review of petro-structural data in the geochronological frame. *Journal of the Virtual Explorer*, *42*(1). https://doi.org/10.3809/jvirtex.2011.00270

Campbell-Stone, E., John, B. E., Foster, D. A., Geissman, J. W., & Livaccari, R. F. (2000). Mechanisms for accommodation of Miocene extension: Low-angle normal faulting, magmatism, and secondary breakaway faulting in the southern Sacramento Mountains, southeastern California. *Tectonics*, *19*, 566–587. https://doi.org/10.1029/10191099TC001133

Cao, S., Neubauer, F., Bernroider, M., Genser, J., Liu, J., & Friedl, G. (2017). Low-grade retrogression of a high-temperature metamorphic core complex: Naxos, Cyclades, Greece. *Geological Society of America Bulletin*, *129*(1–2), 93–117. https://doi.org/10.1130/B31502.31501

Cao, S., Neubauer, F., Bernroider, M., & Liu, J. (2013). The lateral boundary of a metamorphic core complex: The Moutsounas shear zone on Naxos, Cyclades, Greece. *Journal of Structural Geology*, *54*, 103–128. https://doi.org/10.1016/j.jsg.2013.1007.1002

Carr, S. D. (1992). Tectonic setting and U-Pb geochronology of the Early Tertiary Ladybird Leucogranite Suite, Thor-Odin - Pinnacles Area, Southern Omineca Belt, British Columbia. *Tectonics*, *11*, 258–278. https://doi.org/10.1029/1091TC01644

Charles, N., Augier, R., Gumiaux, C., Monie, P., Chen, Y., Faure, M., & Zhu, R. (2013). Timing, duration and role of magmatism in wide rift systems: Insights from the Jiaodong Peninsula (China, East Asia). *Gondwana Research*, *24*(1), 412–428. https://doi.org/10.1016/j.gr.2012.1010.1011

Charles, N., Gumiaux, C., Augier, R., Chen, Y., Zhu, R., & Lin, W. (2011). Metamorphic core complexes vs. synkinematic plutons in continental extension setting: Insights from key structures (Shandong Province, eastern China). *Journal of Asian Earth Sciences*, *40*, 261–278. https://doi.org/10.1016/j.jseaes.2010.1007.1006

Coney, P. J., & Harms, T. A. (1984). Cordilleran metamorphic core complexes, Cenozoic extensional relics of Mesozoic compression. *Geology*, *12*, 550–554. https://doi.org/10.1130/0091%E2%80%937613(1984)1112%3C1550:CMCCCE%3E1132.1130.CO;1132

Cossette, E., Schneider, D. A., Warren, C. J., & Grasemann, B. (2015). Lithological, rheological, and fluid infiltration control on $^{40}Ar/^{39}Ar$ ages in polydeformed rocks from the West Cycladic detachment system, Greece. *Lithosphere*, *7*(2), 189–205. https://doi.org/10.1130/L1416.1131

Crittenden, M. D., Coney, P. J., & Davis, G. H. (1980). Cordilleran metamorphic core complexes. *Geological Society of America Memoirs*, *153*, 1–490.

Dabrowski, M., & Grasemann, B. (2014). Domino boudinage under layer-parallel simple shear. *Journal of Structural Geology*, *68*, 58–65. https://doi.org/10.1016/j.jsg.2014.1009.1006

Dallmeyer, R. D., Snoke, A. W., & McKee, E. M. (1986). The Mesozoic-Cenozoic tectonothermal evolution of the Ruby Mountains, East Humboldt Range, Nevada: A Cordilleran Metamorphic Core Complex. *Tectonics*, *5*(6), 931–954. https://doi.org/10.1029/TC10201005i1006p00931

Daniel, J. M., & Jolivet, L. (1995). Detachment faults and pluton emplacement; Elba Island (Tyrrhenian Sea). *Bulletin de la Societe Geologique de France*, *166*(4), 341–354.

Davis, G. A., Fowler, T. K., Bishop, K. M., Brudos, T. C., Friedmann, S. J., Burbank, D. W., et al. (1993). Pluton pinning of an active Miocene detachment fault system, eastern Mojave Desert, California. *Geology*, *21*(7), 627–630. https://doi.org/10.1130/0091–7613(1993)1021<0627:PPOAAM>1132.1133.CO;1132

Davis, G. A., Qian, X., Zheng, Y., Yu, H., Wang, C., Mao, T. H., et al. (1996). Mesozoic deformation and plutonism in the Yunmeng Shan: A Chinese metamorphic core complex north of Beijing, China. In *The tectonic evolution of Asia* (pp. 253–280). Cambridge: Cambridge University Press.

Davis, G. H., & Coney, P. J. (1979). Geologic development of the Cordilleran metamorphic core complexes. *Geology*, *7*(3), 120–124. https://doi.org/10.1130/0091–7613(1979)1137<1120:GDOTCM>1132.1130.CO;1132

Denèle, Y., Lecomte, E., Jolivet, L., Lacombe, O., Labrousse, L., Huet, B., & Le Pourhiet, L. (2011). Granite intrusion in a metamorphic core complex: The example of the Mykonos laccolith (Cyclades, Greece). *Tectonophysics*, *501*(1-4), 52–70. https://doi.org/10.1016/j.tecto.2011.1001.1013

Dimitriadis, I., Karagianni, E., Panagiotopoulos, D., Papazachos, C., Hatzidimitriou, P., Bohnhoff, M., et al. (2009). Seismicity and active tectonics at Coloumbo Reef (Aegean Sea, Greece): Monitoring an active volcano at Santorini Volcanic Center using a temporary seismic network. *Tectonophysics*, *465*(1–4), 136–149. https://doi.org/10.1016/j.tecto.2008.1011.1005

Dimitriadis, I., Papazachos, C., Panagiotopoulos, D., Hatzidimitriou, P., Bohnhoff, M., Rische, M., & Meier, T. (2010). P and S velocity structures of the Santorini–Coloumbo volcanic system (Aegean Sea, Greece) obtained by non-linear inversion of travel times and its tectonic implications. *Journal of Volcanology and Geothermal Research*, *195*(1), 13–30. https://doi.org/10.1016/j.jvolgeores.2010.1005.1013

Dinter, D. A., & Royden, L. (1993). Late Cenozoic extension in northeastern Greece: Strymon valley detachment system and Rhodope metamorphic core complex. *Geology*, *21*(1), 45–48. https://doi.org/10.1130/0091-7613(1993)1021<0045:LCEING>1132.1133.CO;1132

Dürr, S., Altherr, R., Keller, J., Okrusch, M., & Seidel, E. (1978). The median Aegean crystalline belt: Stratigraphy, structure, metamorphism, magmatism. In H. Cloos, D. Roeder, & K. Schmidt (Eds.), *Alps, Appenines, Hellenides* (pp. 455–477). Stuttgart: Schweizerbart.

Ersoy, E. Y., & Palmer, M. R. (2013). Eocene-Quaternary magmatic activity in the Aegean: Implications for mantle metasomatism and magma genesis in an evolving orogeny. *Lithos*, *180-181*, 5–24. https://doi.org/10.1016/j.lithos.2013.1006.1007

Rossetti, F., Faccenna, C., Jolivet, L., & Funiciello, R. (1999). Structural evolution of the Giglio island, Northern Tyrrhenian Sea (Italy). *Memorie Della Societa' Geologica Italiana*, *52*, 493–512.

Famin, V. (2003). Incursion de fluides dans une zone de cisaillement ductile (Tinos, Cyclades, Grèce): mécanismes de circulation et implications tectoniques, (Thèse de Doctorat thesis, 296 pp.). Paris: Université Pierre et Marie Curie.

Faure, M., Bonneau, M., & Pons, J. (1991). Ductile deformation and syntectonic granite emplacement during the late Miocene extension of the Aegean (Greece). *Bulletin de la Societe Geologique de France*, *162*, 3–12.

Faure, M., Sun, Y., Shu, L., Monié, P., & Charvet, J. (1996). Extensional tectonics within a subduction-type orogen. The case study of the Wugongshan dome (Jiangxi Province, southeastern China). *Tectonophysics*, *263*(1–4), 77–106. https://doi.org/10.1016/S0040–1951(1097)81487–81484

Fletcher, J. M., Bartley, J. M., Martin, M. W., Glazner, A. F., & Walker, J. D. (1995). Large-magnitude continental extension: An example from the central Mojave metamorphic core complex. *Geological Society of America Bulletin*, *107*(12), 1468–1483. https://doi.org/10.1130/0016–7606(1995)1107<14141468:LMCEAE>1462.1463.CO;1462

Foster, M., & Lister, G. (2009). Core-complex-related extension of the Aegean lithosphere initiated at the Eocene-Oligocene transition. *Journal of Geophysical Research*, *114*, B02401. https://doi.org/10.01029/02007JB005382Click

Gans, P. B. (1987). An open system, two layer crustal stretching model for the eastern Great Basin. *Tectonics*, *6*, 1–12. https://doi.org/10.1029/TC1006i1001p00001

Gautier, P., & Brun, J. P. (1994a). Crustal-scale geometry and kinematics of late-orogenic extension in the central Aegean (Cyclades and Evvia island). *Tectonophysics*, *238*, 399–424. https://doi.org/10.1016/0040–1951(1094)90066–90063

Gautier, P., & Brun, J. P. (1994b). Ductile crust exhumation and extensional detachments in the central Aegean (Cyclades and Evvia islands). *Geodinamica Acta*, *7*(2), 57–85. https://doi.org/10.1080/09853111.1994.11105259

Gautier, P., Brun, J. P., & Jolivet, L. (1993). Structure and kinematics of upper Cenozoic extensional detachement on Naxos and Paros (Cyclades Islands, Greece). *Tectonics*, *12*, 1180–1194. https://doi.org/10.1029/1193TC01131

Goldsworthy, M., Jackson, J., & Haines, J. (2002). The continuity of active fault systems in Greece. *Geophysical Journal International*, *148*, 596–618. https://doi.org/10.1046/j.1365-1246X.2002.01609.x

Grasemann, B., & Petrakakis, K. (2007). Evolution of the Serifos metamorphic core complex. *Journal of the Virtual Explorer*, *27*, 1–18.

Grasemann, B., Schneider, D. A., Stockli, D. F., & Iglseder, C. (2012). Miocene bivergent crustal extension in the Aegean: Evidence from the western Cyclades (Greece). *Lithosphere*, *4*(1), 23–39. https://doi.org/10.1130/L1164.1131

Grasemann, B., & Tschegg, C. (2012). Localization of deformation triggered by chemo-mechanical feedback processes. *Geological Society of America Bulletin*, *124*(5–6), 737–745. https://doi.org/10.1130/B30504.30501

Groppo, C., Forster, M., Lister, G., & Compagnoni, R. (2009). Glaucophane schists and associated rocks from Sifnos (Cyclades, Greece): New constraints on the P–T evolution from oxidized systems. *Lithos*, *109*(3–4), 254–273. https://doi.org/10.1016/j.lithos.2008.1010.1005

Habert, G. (2004). Etude des relations entre la structure des granites et le contexte tectonique: exemple des contextes transpressifs, extensifs et sans tectonique, (Thèse de Doctorat thesis, 326 pp.). Toulouse: Université de Toulouse III - Paul Sabatier.

Hatzfeld, D., Karakostas, V., Ziazia, M., Kassaras, I., Papadimitriou, E., Makropoulos, K., et al. (2000). Microseismicity and faulting geometry in the Gulf of Corinth (Greece). *Geophysical Journal International*, *141*, 438–456. https://doi.org/10.1046/j.1365-1246x.2000.00092.x

Hejl, E., Riedl, H., & Weingartner, H. (2002). Post-plutonic unroofing and morphogenesis of the Attic-Cycladic complex (Aegea, Greece). *Tectonophysics*, *349*(1-4), 37–56. https://doi.org/10.1016/S0040-1951(1002)00045-00048

Henjes-Kunst, F., & Kreuzer, H. (1982). Isotopic dating of pre-alpidic rocks from the Island of Ios (Cyclades, Greece). *Contributions to Mineralogy and Petrology*, *80*, 245–253. https://doi.org/10.1007/BF00371354

Hetzel, R., Passchier, C. W., Ring, U., & Dora, O. O. (1995). Bivergent extension in orogenic belts: The Menderes massif (southwestern Turkey). *Geology*, *23*(5), 455–458. https://doi.org/10.1130/0091-7613(1995)023<0455:BEIOBT>2.3.CO;2

Hezel, D. C., Kalt, A., Marschall, H. R., Ludwig, T., & Meyer, H. P. (2011). Major-element and Li, Be compositional evolution of tourmaline in an S-type granite-pegmatite system and its country rocks: An example from Ikaria, Aegean Sea, Greece. *The Canadian Mineralogist*, *49*(1), 321–340. https://doi.org/10.3749/canmin.3749.3741.3321

Hill, E. J., Baldwin, S. L., & Lister, G. S. (1995). Magmatism as an essential driving force for formation of active metamorphic core complexes in eastern Papua New Guinea. *Journal of Geophysical Research*, *100*, 10,441–10,451. https://doi.org/10.11029/10494JB03329

Huet, B., Labrousse, L., & Jolivet, L. (2009). Thrust or detachment? Exhumation processes in the Aegean: insight from a field study on Ios (Cyclades, Greece). *Tectonics*, *28*, TC3007. https://doi.org/10.1029/2008TC002397

Huet, B., Labrousse, L., Monié, P., Malvoisin, B., & Jolivet, L. (2015). Coupled phengite ^{40}Ar-^{39}Ar geochronology and thermobarometry: P-T-t evolution of Andros Island (Cyclades, Greece). *Geological Magazine*, *152*(4), 711–727. https://doi.org/10.1017/S0016756814000661

Hyndman, D. W. (1980). Bitterroot dome-sapphire tectonic block, an example of a plutonic-core gneiss-dome complex with its detached suprastructure. *Geological Society of America Memoirs*, *153*, 427–444. https://doi.org/10.1130/MEM153-p427

Iglseder, C., Grasemann, B., Rice, A. H. N., Petrakakis, K., & Schneider, D. A. (2011). Miocene south directed low-angle normal fault evolution on Kea (West Cycladic Detachment System, Greece). *Tectonics*, *30*, TC4013. https://doi.org/10.1029/2010TC002802

Iglseder, C., Grasemann, B., Schneider, D. A., Petrakakis, K., Miller, C., Klötzli, U. S., et al. (2009). I and S-type plutonism on Serifos (W-Cyclades, Greece). *Tectonophysics*, *473*(1-2), 69–83. https://doi.org/10.1016/j.tecto.2008.1009.1021

Jackson, J. (1994). Active tectonics of the Aegean region. *Annual Review of Earth and Planetary Sciences*, *22*, 239–271. https://doi.org/10.1146/annurev.earth.1122.1141.1239

Jacobshagen, V., Dürr, S., Kockel, F., Kopp, K. O., Kowalczyk, G., Berckhemer, H., & Büttner, D. (1978). Structure and geodynamic evolution of the Aegean region. In H. Cloos, D. Roeder, & K. Schmidt (Eds.), *Alps, Apennines, Hellenides* (pp. 537–564). Stuttgart: IUGG.

Jansen, J. B. H. (1973). *Geological map of Naxos (1/50 000), Nation*. Athens: Inst. Geol. Mining Res.

Jansen, J. B. H. (1977). Metamorphism on Naxos, Greece, (PhD thesis). Utrecht University, Netherlands.

Jansen, J. B. H., & Schuilling, R. (1976). Metamorphism on Naxos: Petrology and geothermal gradient. *American Journal of Science*, *276*(10), 1225–1253. https://doi.org/10.2475/ajs.276.10.1225

John, B. E., & Howard, K. A. (1995). Rapid extension recorded by cooling-age patterns and brittle deformation, Naxos, Greece. *Journal of Geophysical Research*, *100*, 9969–9979. https://doi.org/10.1029/9995JB00665

Jolivet, L. (2001). A comparison of geodetic and finite strain in the Aegean, geodynamic implications. *Earth and Planetary Science Letters*, *187*, 95–104. https://doi.org/10.1016/S0012-1821X(1001)00277–00271

Jolivet, L., & Brun, J. P. (2010). Cenozoic geodynamic evolution of the Aegean region. *International Journal of Earth Sciences*, *99*, 109–138. https://doi.org/10.1007/s00531–00008–00366-00534

Jolivet, L., Daniel, J. M., Truffert, C., & Goffé, B. (1994). Exhumation of deep crustal metamorphic rocks and crustal extension in back-arc regions. *Lithos*, *33*(1-3), 3–30. https://doi.org/10.1016/0024-4937(1094)90051-90055

Jolivet, L., Dubois, R., Fournier, M., Goffé, B., Michard, A., & Jourdan, C. (1990). Ductile extension in Alpine Corsica. *Geology*, *18*(10), 1007–1010. https://doi.org/10.1130/0091-7613(1990)018<1007:DEIAC>2.3.CO;2

Jolivet, L., & Faccenna, C. (2000). Mediterranean extension and the Africa-Eurasia collision. *Tectonics*, *19*(6), 1095–1106. https://doi.org/10.1029/2000TC900018

Jolivet, L., Faccenna, C., Goffé, B., Burov, E., & Agard, P. (2003). Subduction tectonics and exhumation of high-pressure metamorphic rocks in the Mediterranean orogens. *American Journal of Science*, *303*, 353–409. https://doi.org/10.2475/ajs.2303.2475.2353

Jolivet, L., Faccenna, C., Goffé, B., Mattei, M., Rossetti, F., Brunet, C., et al. (1998). Mid-crustal shear zones in post-orogenic extension: the northern Tyrrhenian Sea case. *Journal of Geophysical Research*, *103*, 12,123–12,160. https://doi.org/10.11029/12197JB03616

Jolivet, L., Faccenna, C., Huet, B., Labrousse, L., le Pourhiet, L., Lacombe, O., et al. (2013). Aegean tectonics: Progressive strain localisation, slab tearing and trench retreat. *Tectonophysics*, *597-598*, 1–33. https://doi.org/10.1016/j.tecto.2012.1006.1011

Jolivet, L., Faccenna, C., & Piromallo, C. (2009). From mantle to crust: Stretching the Mediterranean. *Earth and Planetary Science Letters*, *285*, 198–209. https://doi.org/10.1016/j.epsl.2009.1006.1017

Jolivet, L., Famin, V., Mehl, C., Parra, T., Aubourg, C., Hébert, R., & Philippot, P. (2004). Strain localization during crustal-scale boudinage to form extensional metamorphic domes in the Aegean Sea. In D. L. Whitney, C. Teyssier, & C. S. Siddoway (Eds.), *Gneiss domes in orogeny* (pp. 185–210). Boulder, CO: Geological Society of America. https://doi.org/10.1130/0-8137-2380-9.185

Jolivet, L., Lecomte, E., Huet, B., Denèle, Y., Lacombe, O., Labrousse, L., et al. (2010). The North Cycladic Detachment System. *Earth and Planetary Science Letters*, *289*, 87–104. https://doi.org/10.1016/j.epsl.2009.1010.1032

Jolivet, L., Maluski, H., Beyssac, O., Goffé, B., Lepvrier, C., Thi, P. T., & Van Vuong, N. (1999). The Oligo-Miocene Bu Khang extensional gneiss dome in North Vietnam, geodynamic implications. *Geology*, *27*(1), 67–70. https://doi.org/10.1130/0091-7613(1999)027<0067:OMBKEG>2.3.CO;2

Jolivet, L., Menant, A., Sternai, P., Rabillard, A., Arbaret, L., Augier, R., et al. (2015). The geological signature of a slab tear below the Aegean. *Tectonophysics*, *659*, 166–182. https://doi.org/10.1016/j.tecto.2015.1008.1004

Jolivet, L., & Patriat, M. (1999). Ductile extension and the formation of the Aegean Sea. In B. Durand, L. Jolivet, F. Horvàth, & M. Séranne (Eds.), *The Mediterranean basins: Tertiary extension within the Alpine orogen* (pp. 427-456). London: Geological Society. https://doi.org/10.1144/GSL.SP.1999.1156.1101.1120

Jolivet, L., Rimmelé, G., Oberhänsli, R., Goffé, B., & Candan, O. (2004). Correlation of syn-orogenic tectonic and metamorphic events in the Cyclades, the Lycian Nappes and the Menderes massif, geodynamic implications. *Bulletin de la Societe Geologique de France*, *175*(3), 217–238. https://doi.org/10.2113/2175.2113.2217

Katzir, Y., Matthews, A., Garfunkel, Z., Schliestedt, M., & Avigad, D. (1996). The tectono-metamorphic evolution of a dismembered ophiolite (Tinos, Cyclades, Greece). *Geological Magazine*, *133*(03), 237–254. https://doi.org/10.1017/S0016756800008992

Keay, S. (1998). The geological evolution of the Cyclades, Greece, constraints from SHRIMP U/Pb geochronology, Australian National University, Cambera, Australia.

Keay, S., & Lister, G. (2002). African provenance for the metasediments and metaigneous rocks of the Cyclades, Aegean Sea, Greece. *Geology*, *30*(3), 235–238. https://doi.org/10.1130/0091–7613(2002)1030<0235:APFTMA>1132.1130.CO;1132

Keay, S., Lister, G., & Buick, I. (2001). The timing of partial melting, Barrovian metamorphism and granite intrusion in the Naxos metamorphic core complex, Cyclades, Aegean Sea, Greece. *Tectonophysics*, *342*, 275–312. https://doi.org/10.1016/S0040–1951(1001)00168–00168

Keiter, M., Piepjohn, K., Ballhaus, C., Lagos, M., & Bode, M. (2004). Structural development of high-pressure metamorphic rocks on Syros island (Cyclades, Greece). *Journal of Structural Geology*, *26*, 1433–1445. https://doi.org/10.1016/j.jsg.2003.1411.1027

Kokkalas, S., & Aydin, A. (2013). Is there a link between faulting and magmatism in the south-central Aegean Sea? *Geological Magazine*, *150*(2), 193–224. https://doi.org/10.1017/S0016756812000453

Koukouvelas, I. K., & Kokkalas, S. (2003). Emplacement of the Miocene west Naxos pluton (Aegean Sea, Geece): A structural study. *Geological Magazine*, *140*(1), 45–61. https://doi.org/10.1017/S0016756802007094

Krohe, A., Mposkos, E., Diamantopoulos, A., & Kaouras, G. (2010). Formation of basins and mountain ranges in Attica (Greece): The role of Miocene to Recent low-angle normal detachment faults. *Earth-Science Reviews*, *98*(1–2), 81–104. https://doi.org/10.1016/j.earscirev.2009.1010.1005

Kruckenberg, S. C. (2009). The dynamics of migmatite domes in extending orogens, (PhD thesis). University of Minnesota, Minneapolis, U.S.A.

Kruckenberg, S. C., Vanderhaeghe, O., Ferré, E. C., Teyssier, C., & Whitney, D. L. (2011). Flow of partially molten crust and the internal dynamics of a migmatite dome, Naxos, Greece: Internal dynamics of the Naxos dome. *Tectonics*, *30*, TC3001. https://doi.org/10.1029/2010TC002751

Kuhlemann, J., Frisch, W., Dunkl, I., Kázmér, M., & Schmiedl, G. (2004). Miocene siliciclastic deposits of Naxos Island: Geodynamic and environmental implications for the evolution of the southern Aegean Sea (Greece). In M. Bernet & C. Spiegel (Eds.), *Detrital thermochronology—Provenance analysis, exhumation, and landscape evolution of mountain belts* (pp. 51–65). Boulder, CO: Geological Society of America.

Kumerics, C., Ring, U., Brichau, S., Glodny, J., & Monié, P. (2005). The extensional Messaria shear zone and associated brittle detachment faults, Aegean Sea, Greece. *Journal of the Geological Society*, *162*(4), 701–721. https://doi.org/10.1144/0016–764904-764041

Lacombe, O., Jolivet, L., Le Pourhiet, L., Lecomte, E., & Mehl, C. (2013). Initiation, geometry and mechanics of brittle faulting in exhuming metamorphic rocks: Insights from the northern Cycladic islands (Aegean, Greece). *Bulletin de la Société Géologique de France*, *184*, 383–403 . https://doi.org/10.2113/gssgfbull.2184.2114–2115.2383

Laurent, V., Beaudoin, A., Jolivet, L., Arbaret, L., Augier, R., & Rabillard, A. (2015). Interrelations between extensional shear zones and synkinematic intrusions: The example of Ikaria Island (NE Cyclades, Greece). *Tectonophysics*, *651-652*, 152–171. https://doi.org/10.1016/j.tecto.2015.1003.1020

Laurent, V., Huet, B., Labrousse, L., Jolivet, L., Monié, P., & Augier, R. (2017). Extraneous argon in high-pressure metamorphic rocks: Distribution, origin and transport in the Cycladic Blueschist Unit (Greece). *Lithos*, *272–273*, 315–335. https://doi.org/10.1016/j.lithos.2016.1012.1013

Laurent, V., Jolivet, L., Roche, V., Augier, R., Scaillet, S., & Cardello, L. (2016). Strain localization in a fossilized subduction channel: Insights from the Cycladic Blueschist Unit (Syros, Greece). *Tectonophysics*, *672-673*, 150–169. https://doi.org/10.1016/j.tecto.2016.1001.1036

Le Pichon, X., & Angelier, J. (1981a). The Aegean Sea. *Philosophical Transactions. Royal Society of London*, *300*(1454), 357–372. https://doi.org/10.1098/rsta.1981.0069

Le Pichon, X., & Angelier, J. (1981b). The Hellenic arc and trench system: A key to the neotectonic evolution of the eastern mediterranean area. *Philosophical Transactions. Royal Society of London*, *300*, 357–372.

Lecomte, E., Jolivet, L., Lacombe, O., Denèle, Y., Labrousse, L., & Le Pourhiet, L. (2010). Geometry and kinematics of a low-angle normal fault on Mykonos island (Cyclades, Greece): Evidence for slip at shallow dip. *Tectonics*, *29*, TC5012. https://doi.org/10.1029/2009TC002564

Lecomte, E., Le Pourhiet, L., Lacombe, O., & Jolivet, L. (2011). A continuum mechanics approach to quantify brittle strain on weak faults: Application to the extensional reactivation of shallow-dipping discontinuities. *Geophysical Journal International*, *184*(1), 1–11. https://doi.org/10.1111/j.1365-1246X.2010.04821.x

Lee, J., & Lister, G. S. (1992). Late Miocene ductile extension and detachment faulting, Mykonos, Greece. *Geology*, *20*, 121–124. https://doi.org/10.1130/0091–7613(1992)1020<0121:LMDEAD>1132.1133.CO;1132

Lekkas, S., Skourtsos, E., Soukis, K., Kranis, H., Lozios, S., Alexopoulos, A., & Koutsovitis, P. (2011). Late Miocene detachment faulting and crustal extension in SE Attica (Greece). *Geophysical Research Abstracts*, *13*, EGU2011–EGU13016.

Lin, W., & Wang, Q. (2006). Late Mesozoic extensional tectonics in the North China block: A crustal response to subcontinental mantle removal? *Bulletin de la Société Géologique de France*, *177*(6), 287–297. https://doi.org/10.2113/gssgfbull.2177.2116.2287

Lister, G. S., & Baldwin, S. (1993). Plutonism and the origin of metamorphic core complexes. *Geology*, *21*, 607–610. https://doi.org/10.1130/0091–7613(1993)1021<0607:PATOOM>1132.1133.CO;1132

Lister, G. S., Banga, G., & Feenstra, A. (1984). Metamorphic core complexes of cordilleran type in the Cyclades, Aegean Sea, Greece. *Geology*, *12*, 221–225. https://doi.org/10.1130/0091–7613(1984)1112<1221:MCCOCT>1132.1130.CO;1132

Lister, G. S., & Davis, G. A. (1989). The origin of metamorphic core complexes and detachment faults formed during Tertiary continental extension in the northern Colorado River region, U.S.A. *Journal of Structural Geology*, *11*(1-2), 65–94. https://doi.org/10.1016/0191-8141(1089)90036-90039

Lucas, I. (1999), Le pluton de Mykonos-Delos-Rhenee (Cyclades, Grèce): un exemple de mise en place synchrone de l'extension crustale (491 pp), Université d'orléans, Orléans.

Lynch, H. D., & Morgan, P. (1987). The tensile strength of the lithosphere and the localization of extension. *Geological Society, London, Special Publications*, *28*(1), 53–65. https://doi.org/10.1144/GSL.SP.11411987.1028.1101.1105

MacCready, T., Snoke, A. W., Wright, J. E., & Howard, K. A. (1997). Mid-crustal flow during Tertiary extension in the Ruby Mountains core complex, Nevada. *Geological Society of America Bulletin*, *109*(12), 1576–1594. https://doi.org/10.1130/0016–7606(1997)1109<1576:MCFDTE>1572.1573.CO;1572

Maluski, H., Bonneau, M., & Kienast, J. R. (1987). Dating the metamorphic events in the Cycladic area: $^{39}Ar/^{40}Ar$ data from metamorphic rocks of the island of Syros (Greece). *Bulletin de la Societe Geologique de France*, *8*, 833–842.

Martha, S. O., Dörr, W., Gerdes, A., Petschick, R., Schastok, J., Xypolias, P., & Zulauf, G. (2016). New structural and U–Pb zircon data from Anafi crystalline basement (Cyclades, Greece): Constraints on the evolution of a Late Cretaceous magmatic arc in the Internal Hellenides. *International Journal of Earth Sciences*, *105*(7), 2031–2060. https://doi.org/10.1007/s00531–00016–01346-00538

Martin, L. (2004), Signification des âges U-Pb sur zircon dans l'histoire métamorphique de Naxos et Ikaria (Cyclades, Grèce), (Thèse de Doctorat thesis, 266 pp.). Nancy, France: Université Henri Poincaré.

Martin, L., Duchêne, S., Deloule, E., & Vanderhaeghe, O. (2006). The isotopic composition of zircon and garnet: A record of the metamorphic history of Naxos, Greece. *Lithos*, *87*(3–4), 174–192. https://doi.org/10.1016/j.lithos.2005.1006.1016

Mehl, C., Jolivet, L., & Lacombe, O. (2005). From ductile to brittle: Evolution and localization of deformation below a crustal detachment (Tinos, Cyclades, Greece). *Tectonics*, *24*, TC4017. https://doi.org/10.1029/2004TC001767

Melidonis, M. G. (1980). The geology of Greece: The geological structure and mineral deposits of Tinos island (Cyclades, Greece). *Institute of Geology and Mineral Exploration, Athens*, *13*, 1–80.

Melidonis, N., and M. Triantaphyllis (2003), Geological map of Greece, Tinos-Yaros Islands (1: 50 000), Athens : Institute of Geology and Mineral Exploration (IGME).

Menant, A., Jolivet, L., Augier, R., & Skarpelis, N. (2013). The North Cycladic Detachment System and associated mineralization, Mykonos, Greece: Insights on the evolution of the Aegean domain. *Tectonics*, *32*, 433–452. https://doi.org/10.1002/tect.20037

Menant, A., Jolivet, L., & Vrielynck, B. (2016). Kinematic reconstructions and magmatic evolution illuminating crustal and mantle dynamics of the eastern Mediterranean region since the late Cretaceous. *Tectonophysics*, *675*, 103–140. https://doi.org/10.1016/j.tecto.2016.1003.1007

Menant, A., Sternai, P., Jolivet, L., Guillou-Frottier, L., & Gerya, T. (2016). 3D numerical modeling of mantle flow, crustal dynamics and magma genesis associated with slab roll-back and tearing: The eastern Mediterranean case. *Earth and Planetary Science Letters*, *442*, 93–107. https://doi.org/10.1016/j.epsl.2016.1003.1002

Papanikolaou, D. (2009). Timing of tectonic emplacement of the ophiolites and terrane paleogeography in the Hellenides. *Lithos*, *108*(1–4), 262–280. https://doi.org/10.1016/j.lithos.10121008.1008.1003

Parra, T., Vidal, O., & Jolivet, L. (2002). Relation between deformation and retrogression in blueschist metapelites of Tinos island (Greece) evidenced by chlorite-mica local equilibria. *Lithos*, *63*(1-2), 41–66. https://doi.org/10.1016/S0024-4937(1002)00115-00119

Parsons, T., & Thompson, G. A. (1993). Does magmatism influence low-angle normal faulting? *Geology*, *21*(3), 247–250. https://doi.org/10.1130/0091–7613(1993)1021<0247:DMILAN>1132.1133.CO;1132

Paterson, S. R., Fowler, T. K., Schmidt, K. L., Yoshinobu, A. S., Yuan, E. S., & Miller, R. B. (1998). Interpreting magmatic fabric patterns in plutons. *Lithos*, *44*(1–2), 53–82. https://doi.org/10.1016/S0024-4937(1098)00022-X

Paterson, S. R., Vernon, R. H., & Tobisch, O. T. (1989). A review of criteria for the identification of magmatic and tectonic foliations in granitoids. *Journal of Structural Geology*, *11*(3), 349–363. https://doi.org/10.1016/0191–8141(1089)90074–90076

Patriat, M., & Jolivet, L. (1998). Post-orogenic extension and shallow-dipping shear zones, study of a brecciated decollement horizon in Tinos (Cyclades, Greece). *Comptes Rendus Mathematique Academie des Sciences, Paris*, *326*, 355–362. https://doi.org/10.1016/S1251–8050(1098)80306–80306

Patzak, M., Okrusch, M., & Kreuzer, H. (1994). The Akrotiri unit on the island of Tinos, Cyclades, Greece: Witness of a lost terrane of Late Cretaceous age. *Neues Jahrbuch für Geologie und Paläontologie Abhandlungen*, *194*, 211–252.

Pavlis, T. L. (1996). Fabric development in syn-tectonic intrusive sheets as a consequence of melt-dominated flow and thermal softening of the crust. *Tectonophysics*, *253*(1–2), 1–31. https://doi.org/10.1016/0040-1951(95)00049-6

Peillod, A., Ring, U., Glodny, J., & Skelton, A. (2017). An Eocene/oligocene blueschist-/greenschist-facies P-T loop from the Cycladic blueschist unit on Naxos Island, Greece: Deformation-related reequilibration vs thermal relaxation. *Journal of Metamorphic Geology*, *35*(7), 805–830. https://doi.org/10.1111/jmg.12256

Pe-Piper, G. (2000). Origin of S-type granites coeval with I-type granites in the Hellenic subduction system, Miocene of Naxos, Greece. *European Journal of Mineralogy*, *12*(4), 859–875. https://doi.org/10.1127/ejm/1112/1124/0859

Pe-Piper, G., NKotopouli, C., & Piper, D. J. W. (1997). Granitoid rocks of Naxos, Greece: regional geology and petrology. *Geological Journal*, *32*(2), 153–171. https://doi.org/10.1002/(SICI)1099–1034(199706)199732:199702<199153::AID-GJ199737>199703.199700.CO;199702–199701

Pe-Piper, G., & Piper, D. J. W. (2006). Unique features of the Cenozoic igneous rocks of Greece. In Y. Dilek & S. Pavlides (Eds.), *Postcollisional tectonics and magmatism in the Mediterranean region and Asia* (pp. 259–282). Boulder, CO: Geological Society of America. https://doi.org/10.1130/2006.2409(1114)

Pe-Piper, G., Piper, D. J. W., & Matarangas, D. (2002). Regional implications of geochemistry and style of emplacement of Miocene I-type diorite and granite, Delos, Cyclades, Greece. *Lithos*, *60*(1–2), 47–66. https://doi.org/10.1016/S0024-4937(1001)00068-00068

Petrakakis, K., Iglseder, C., Zámolyi, A., Rambousek, C., Grasemann, B., Draganitis, E., Kurka, A., & Photiades, A. (2010), Serifos island, Institute of Geology and Mineral Exploration (IGME).

Photiades, A. (2005). Ikaria Island sheet (1: 50 000), Athens : Institute of Geology and Mineral Exploration (IGME).

Platt, J. P., Behr, W. M., & Cooper, F. J. (2015). Metamorphic core complexes: Windows into the mechanics and rheology of the crust. *Journal of the Geological Society, London*, *172*(1), 9–27. https://doi.org/10.1144/jgs2014-1036

Rabillard, A., Arbaret, L., Jolivet, L., Le Breton, N., Gumiaux, C., Augier, R., & Grasemann, B. (2015). Interactions between plutonism and detachments during Metamorphic Core Complex formation, Serifos Island (Cyclades, Greece). *Tectonics*, *34*, 1080–1106. https://doi.org/10.1002/2014TC003650

Reinecke, T., Altherr, R., Hartung, B., Hatzipanagiotou, K., Kreuzer, H., Harre, W., et al. (1982). Remnants of a late Cretaceous high temperature bet on the island of Anafi (Cyclades, Greece). *Neues Jahrbuch für Mineralogie Abhandlungen*, *145*(2), 157–182.

Rice, H. N., Iglseder, C., Grasemann, B., Zámolyi, A., Nikolakopoulos, K. G., Mitropoulos, D., et al. (2012). A new geological map of the crustal-scale detachment on Kea (Western Cyclades, Greece). *Austrian Journal of Earth Sciences*, *105*(3), 108–124.

Ring, U. (2007). The geology of Ikaria Island: The Messaria extensional shear zone, granites and the exotic Ikaria nappe. *Journal of the Virtual Explorer*, *27*(3), 1–32.

Ring, U., Gessner, K., Güngör, T., & Passchier, C. W. (1999). The Menderes massif of western Turkey and the Cycladic massif in the Aegean: Do they really correlate? *Journal of the Geological Society of London*, *156*(1), 3–6. https://doi.org/10.1144/gsjgs.1156.1141.0003

Ring, U., Glodny, J., Will, T., & Thomson, S. (2007). An Oligocene extrusion wedge of blueschists-facies nappes on Evia, Aegean Sea, Greece: implications for the early exhumation of high-pressure rocks. *Journal of the Geological Society of London*, *164*, 637–652. https://doi.org/10.1144/0016–76492006-76492041

Ring, U., Glodny, J., Will, T., & Thomson, S. (2010). The Hellenic subduction system: High-pressure metamorphism, exhumation, normal faulting, and large-scale extension. *Annual Review of Earth and Planetary Sciences*, *38*(1), 45–76, https://doi.org/10.1146/annurev.earth.050708.170910.

Ring, U., Glodny, J., Will, T. M., & Thomson, S. (2011). Normal faulting on Sifnos and the South Cycladic Detachment System, Aegean Sea, Greece. *Journal of the Geological Society, London*, *168*, 751–768. https://doi.org/10.1144/0016–76492010-76492064

Ring, U., Thomson, S. N., & Bröcker, M. (2003). Fast extension but little exhumation: the Vari detachment in the Cyclades, Greece. *Geological Magazine*, *140*(3), 245–252. https://doi.org/10.1017/S0016756803007799

Ring, U., Will, T., Glodny, J., Kumerics, C., Gessner, K., Thomson, S., et al. (2007). Early exhumation of high-pressure rocks in extrusion wedges: Cycladic blueschist unit in the eastern Aegean, Greece, and Turkey. *Tectonics*, *26*, TC2001. https://doi.org/10.1029/2005TC001872

Roche, V., Laurent, V., Cardello, G. L., Jolivet, L., & Scaillet, S. (2016). The anatomy of the Cycladic Blueschist Unit on Sifnos island (Cyclades, Greece). *Journal of Geodynamics*, *97*, 62–87. https://doi.org/10.1016/j.jog.2016.1003.1008

Royden, L. H. (1993). Evolution of retreating subduction boundaries formed during continental collision. *Tectonics*, *12*, 629–638. https://doi.org/10.1029/92TC02641

Royden, L. H., & Papanikolaou, D. J. (2011). Slab segmentation and late Cenozoic disruption of the Hellenic arc. *Geochemistry, Geophysics, Geosystems*, *12*, Q03010. https://doi.org/10.01029/02010GC003280

de Saint Blanquat, M., Horsman, M. E., Habert, G., Morgan, S., Vanderhaeghe, O., Law, R., & Tikoff, B. (2011). Multiscale magmatic cyclicity, duration of pluton construction, and the paradoxical relationship between tectonism and plutonism in continental arcs. *Tectonophysics*, *500*(1–4), 20–33. https://doi.org/10.1016/j.tecto.2009.2012.2009

Salemink, J. (1985). Skarn and ore formation at Serifos, Greece, as a consequence of granodiorite intrusion, (PhD thesis thesis). Netherlands: University of Utrecht.

Sanchez-Gomez, M., Avigad, D., & Heiman, A. (2002). Geochronology of clasts in allochthonous Miocene sedimentary sequences on Mykonos and Paros islands: Implications for back-arc extension in the Aegean Sea. *Journal of the Geological Society of London*, *159*(1), 45–60. https://doi.org/10.1144/0016-764901031

Scheffer, C., Vanderhaeghe, O., Lanari, P., Tarantola, A., Ponthus, L., Photiades, A., & France, L. (2016). Syn- to post-orogenic exhumation of metamorphic nappes: Structure and thermobarometry of the western Attic-Cycladic metamorphic complex (Lavrion, Greece). *Journal of Geodynamics*, *96*, 174–193. https://doi.org/10.1016/j.jog.2015.1008.1005

Schneider, D. A., Senkowski, C., Vogel, H., Grasemann, B., Iglseder, C., & Schmitt, A. K. (2011). Eocene tectonometamorphism on Serifos (western Cyclades) deduced from zircon depth-profiling geochronology and mica thermochronology. *Lithos*, *125*, 151–172. https://doi.org/10.1016/j.lithos.2011.1002.1005

Seman, S., Stockli, D. F., & Soukis, K. (2017). The provenance and internal structure of the Cycladic Blueschist Unit revealed by detrital zircon geochronology, Western Cyclades, Greece. *Tectonics*, *36*, 1407–1429. https://doi.org/10.1002/2016TC004378

Seward, D., Vanderhaeghe, O., Siebenaller, L., Thomson, S., Hibsch, C., Zingg, A., et al. (2009). Cenozoic tectonic evolution of Naxos Island through a multi-faceted approach of fission-track analysis. In U. Ring & B. Wernicke (Eds.), *Extending a continent: Architecture, rheology and heat budget* (pp. 179–196). London: Geological Society. https://doi.org/10.1144/SP1321.1149

Shu, L., Sun, Y., Wang, D., Faure, M., Monie, P., & Charvet, J. (1998). Mesozoic doming extensional tectonics of Wugongshan, South China. *Science in China Series D: Earth Sciences*, *41*(6), 601–608. https://doi.org/10.1007/BF02878742

Siebenaller, L. (2008). Circulations fluides au cours de l'effondrement d'un prisme d'accrétion crustal: L'exemple du "Metamorphic Core Complex" de l'Île de Naxos (Cyclades, Grèce), (PhD thesis). Nancy, France: University Henri Poincaré.

Siebenaller, L., Boiron, M. C., Vanderhaeghe, O., Hibsch, C., Jessel, M. W., André-Mayer, A. S., et al. (2013). Fluid record of rock exhumation across the brittle–ductile transition during formation of a Metamorphic Core Complex (Naxos Island, Cyclades, Greece). *Journal of Metamorphic Geology*, *31*, 313–338. https://doi.org/10.1111/jmg.12023

Skarpelis, N. (2007). The Lavrion deposit (SE Attica, Greece): Geology, mineralogy and minor elements chemistry. *Neues Jahrbuch für Mineralogie Abhandlungen*, *183*(3), 227–249. https://doi.org/10.1127/0077–7757/2007/0067

Soukis, K., & Stöckli, D. (2013). Structural and thermochronometric evidence for multi-stage exhumation of Southern Syros, Cycladic Islands, Greece. *Tectonophysics*, *595–596*, 148–164. https://doi.org/10.1016/j.tecto.2012.1005.1017

Spencer, J. E. (1984). Role of tectonic denudation in warping and uplift of low-angle normal faults. *Geology*, *12*(2), 95–98. https://doi.org/10.1130/0091-7613(1984)1112<1195:ROTDIW>1132.1130.CO;1132

St. Seymour, K., Zouzias, D., Tombros, S., & Kolaiti, E. (2009). Geochemistry of the Serifos pluton (Cycladic islands) and associated iron oxide and sulfide ores: Skarn or metamorphosed exhalite deposits? *Neues Jahrbuch für Mineralogie Abhandlungen*, *186*(3), 249–270. https://doi.org/10.1127/0077–7757/2009/0143

Stouraiti, C., Mitropoulos, P., Tarney, J., Barreiro, B., McGrath, A. M., & Baltatzis, E. (2010). Geochemistry and petrogenesis of late Miocene granitoids, Cyclades, southern Aegean: Nature of Sourcesource components. *Lithos*, *114*, 337–352. https://doi.org/10.1016/j.Lithoslithos.2009.1009.1010

Teyssier, C., Ferré, E. C., Whitney, D. L., Norlander, B., Vanderhaeghe, O., & Parkinson, D. (2005). Flow of partially molten crust and origin of detachments during collapse of the Cordilleran Orogen. *Geological Society, London, Special Publications*, *245*(1), 39–64. https://doi.org/10.1144/GSL.SP.2005.1245.1101.1103

Teyssier, C., & Whitney, D. L. (2002). Gneiss domes and orogeny. *Geology*, *30*(12), 1139–1142. https://doi.org/10.1130/0091–7613(2002)1030<1139:GDAO>1132.1130.CO;1132

Trotet, F., Jolivet, L., & Vidal, O. (2001). Tectono-metamorphic evolution of Syros and Sifnos islands (Cyclades, Greece). *Tectonophysics*, *338*(2), 179–206. https://doi.org/10.1016/S0040-1951(01)00138-X

Tschegg, C., & Grasemann, B. (2009). Deformation and alteration of a granodiorite during low-angle normal faulting (Serifos, Greece). *Lithosphere*, *1*(3), 139–154. https://doi.org/10.1130/L1133.1131

Urai, J. L., Shuiling, R. D., & Jansen, J. B. H. (1990). Alpine deformation on Naxos (Greece). In R. J. Knipe & E. H. Rutter (Eds.), *Deformation mechanisms, rheology and Tectonics* (pp. 509–522). London: Geological Society, London, Special Publications. https://doi.org/10.1144/GSL.SP.1990.1054.1101.1147

Vandenberg, L. C., & Lister, G. S. (1996). Structural analysis of basement tectonics from the Aegean metamorphic core complex of Ios, Cyclades, Greece. *Journal of Structural Geology*, *18*(12), 1437–1454. https://doi.org/10.1016/S0191–8141(1496)00068

Vanderhaeghe, O. (1999). Pervasive melt migration from migmatites to leucogranite in the Shuswap metamorphic core complex, Canada: Control of regional deformation. *Tectonophysics*, *312*(1), 35–55. https://doi.org/10.1016/S0040-1951(1099)00171-00177

Vanderhaeghe, O. (2004). Structural development of the Naxos migmatite dome. In D. L. Whitney, C. Teyssier, & C. S. Siddoway (Eds.), *Gneiss domes in orogeny* (pp. 211–227). Boulder, CO: Geological Society of America. https://doi.org/10.1130/0-8137-2380-9.211

Vanderhaeghe, O. (2009). Migmatites, granites and orogeny: Flow modes of partially-molten rocks and magmas associated with melt/solid segregation in orogenic belts. *Tectonophysics*, *477*(3–4), 119–134. https://doi.org/10.1016/j.tecto.2009.1006.1021

Vanderhaeghe, O. (2012). The thermal–mechanical evolution of crustal orogenic belts at convergent plate boundaries: A reappraisal of the orogenic cycle. *Journal of Geodynamics*, *56–57*, 124–145. https://doi.org/10.1016/j.jog.2011.1010.1004

Vanderhaeghe, O., Hibsch, C., Siebenaller, L., Duchêne, S., de St Blanquat, M., Kruckenberg, S., et al. (2007). Penrose conference-extending a continent-Naxos field guide. *Journal of the Virtual Explorer, Electronic Edition*, *27*, 1–23. https://doi.org/10.3809/jvirtex.2007.00175

Vanderhaeghe, O., Hibsch, C., Siebenaller, L., Duchêne, S., Kruckenberg, S., Fotiadis, A., et al. (2007). Penrose conference-extending a continent-Naxos field guide. *Journal of the Virtual Explorer*, *28*, 4.

Vanderhaeghe, O., & Teyssier, C. (1997). Formation of the Shuswap metamorphic core complex during late-orogenic collapse of the Canadian Cordillera: Role of ductile thinning and partial melting of the mid-to lower crust. *Geodinamica Acta*, *10*(2), 41–58. https://doi.org/10.1080/09853111.09851997.11105292

Vanderhaeghe, O., & Teyssier, C. (2001). Partial melting and the flow of orogens. *Tectonophysics*, *342*(3-4), 451–472. https://doi.org/10.1016/S0040–1951(1001)00175–00175

van Hinsbergen, D. J. J., Hafkenscheid, E., Spakman, W., Meulenkamp, J. E., & Wortel, R. (2005). Nappe stacking resulting from subduction of oceanic and continental lithosphere below Greece. *Geology*, *33*(4), 325–328. https://doi.org/10.1130/G20878.20871

Vernon, R. H. (2000). Review of microstructural evidence of magmatic and solid-state flow. *Visual Geosciences*, *5*(2), 1–23. https://doi.org/10.1007/s10069-10000-10002-10063

Vigneresse, J. L., Tikoff, B., & Améglio, L. (1999). Modification of the regional stress field by magma intrusion and formation of tabular granitic plutons. *Tectonophysics*, *302*(3-4), 203–224. https://doi.org/10.1016/S0040-1951(1098)00285-00286

Webb, L. E., Graham, S. A., Johnson, C. L., Badarch, G., & Hendrix, M. S. (1999). Occurrence, age, and implications of the Yagan–Onch Hayrhan metamorphic core complex, southern Mongolia. *Geology*, *27*(2), 143–146. https://doi.org/10.1130/0091–7613(1999)1027<0143:OAAIOT>1132.1133.CO;1132

Whitney, D. L., & Dilek, Y. (1997). Core complex development in central Anatolia, Turkey. *Geology*, *25*(11), 1023–1026. https://doi.org/10.1130/0091%E2%80%937613(1997)1025%3C1023:CCDICA%3E1022.1023.CO;1022

Whitney, D. L., Teyssier, C., Rey, P., & Buck, W. R. (2013). Continental and oceanic core complexes. *Geological Society of America Bulletin*, *125*(3–4), 273–298. https://doi.org/10.1130/B30754.1

Whitney, D. L., Teyssier, C., & Vanderhaeghe, O. (2004). Gneiss domes and crustal flow. In D. L. Whitney, C. Teyssier, & C. S. Siddoway (Eds.), *Gneiss domes in orogeny* (pp. 15–33). Boulder, CO: Geological Society of America. https://doi.org/10.1130/0-8137-2380-9.15

Wijbrans, J. R., & McDougall, I. (1986). $^{40}Ar/^{39}Ar$ dating of white micas from an alpine high-pressure metamorphic belt on Naxos (Greece); The resetting of the argon isotopic system. *Contributions to Mineralogy and Petrology*, *93*(2), 187–194. https://doi.org/10.1007/BF00371320

Wijbrans, J. R., & McDougall, I. (1988). Metamorphic evolution of the Attic Cycladic Metamorphic Belt on Naxos (Cyclades, Greece) utilizing $^{40}Ar/^{39}Ar$ age spectrum measurements. *Journal of Metamorphic Geology*, *6*(5), 571–594. https://doi.org/10.1111/j.1525–1314.1988.tb00441.x

Zeffren, S., Avigad, D., Heimann, A., & Gvirtzman, Z. (2005). Age resetting of hanging wall rocks above a Tertiary low-angle detachment, Tinos island, Aegean Sea. *Tectonophysics*, *400*(1–4), 1–25. https://doi.org/10.101106/j.tecto.2005.2001.2003